C H A P T E R - II

MECHANICAL BEHAVIOUR OF JOINTED ROCKS

2.1.0. GENERAL

The rock essentially is an anisotropic discontinuous mass containing cracks, fissures, joints, faults and bedding planes with varying degree of cohesion along these discontinuities. A number of studies have been conducted in order to evolve some sort of clastic model, in lieu of non realistic and too simplistic continuum models, which can be used for investigating the stability of rocks. Though the studies have yielded very interesting results it has yet not been possible to produce a realistic model. Nevertheless the results of these studies could identify the factors which governs the shearing behaviour of jointed rocks. These factors are: the mechanical behaviour of individual element constituting the system, sliding characteristics of joints, the configuration of the system and the operating stress field. The basic steps for the development of a clastic model have been the extension of classical theory of friction for rock masses by incorporating the behaviour of joints and mathematical formulation of a failure criterion along with a convenient constitutive equation keeping in view the above factors.

2.2.0. THEORY OF FRICTION

2.2.1. Concept of friction

From Vinci's notes (1452-1519) about sliding between the celestial bodies, the concept of friction between the bodies originated and propagated through the experimental work of Amontons (1699) and Coulomb (1785). However, the fundamental understanding as regards the phenomenon of friction between bodies is a result of number of workers from Rayleigh through Reynolds, Hardy and Hardy (1919) to Bowden and Tabor (1950,1964). Rayleigh was first to recognize the influence of the characteristics of liquid interface between the surfaces, consequent upon which the various concepts of friction viz: mechanical interlocking of surface roughness elements, molecular attraction, electrostatic forces and most recent concept of welding and ploughing germinated. While these concepts are centered around the friction and lubrication between metal surfaces however the frictional behaviour between rock surfaces is adoption from the theory of friction for metals and not specifically conceptulized from the first principles. The classical work of Griffith (1921) on brittle materials like glass has been taken as a base for theory of friction in intact rocks considering as a brittle material. The theory of friction particularly jointed rock should necessarily spring from the fundamental plank of Coulomb's frame work.

2.2.2. Classical laws of friction

The classical laws of friction are the out come of

the original works of Leonardo-de-Vinci (1452-1519), Amontons (1699) and Coulomb(1785) which can be stated as under.

(i) Tangential force is directly proportional to the normal load.

(ii) The coefficient of friction is independent of contact area.

(iii) Static coefficient of friction is greater than kinetic friction.

(iv) Coefficient of friction is independent of sliding speed.

These classical laws were considered generally valid and no significant amendment came forth until recently. As a consequence of modern researches, these laws need corrections. The first law is correct only at high pressures whence the actual contact area coincides with the apparent area in magnitude. The second law is valid only for materials such as metals which possess definite yield point. It can never be true for elastic and viscoelastic materials. The third law is not at all observed for any viscoelastic material may it be that they may not be possessing the coefficient of friction at all. The fourth law is not valid for any materials. The studies have pointed out that the coefficient of friction is material dependent. While working on these classical laws of friction it was observed that even the best prepared surfaces are not accurately flat and in contact over the whole area but are infact in contact only at small protruderances or asperities. The normal stress at these contacts is very great and will exceed the yield

stress of the softer material. It is also found that if the shearing force is increased steadily some irrerversible displacement takes place at forces less than those necessary to cause slip. The further effects which is studied exclusively for metals is the separation of frictional force into so called shearing and ploughing stresses. Macroscopically in case of irregular surface it may happen that the sliding takes place up a plane inclined at a small angle to the direction of force. With all these events the phenomenon of friction should appear much more complicated. Archard (1958) has discussed the details of various processes more fully and concludes that the law of friction may best be expressed by a power law.

$$F = \mu_0 W^m \qquad \ldots.2.2.1$$

Where $2/3 < m < 1$. The case of $m = 2/3$ corresponds to purely elastic contact in which the area of contact is propartional to $W^{2/3}$.

2.2.3. Friction in jointed rocks

The validity of concepts of plastic flow and welding for metals can not be extended to friction in jointed rocks, only perhaps the concept of contact at limited number of asperities may be of value in understanding the friction phenomenon in jointed rocks. Byerlee (1967 a) conceptulized a model for asperities in the form of a truncated cone and analysised the failure of the asperities by tensile fracture which yielded into a conclusion that the Amontons law may hold true for a single asperity having a small value of μ of the order of 0,1. The observed higher values of μ in practice

is attributed to the interlocking of the asperities. In case of actual rocks the surfaces could be much more irregular and it would be necessary to consider the effect of ploughing of irregular surfaces. Bowden (1954) working on diamond to diamond contacts concluded that the frictional force is proportional to $W^{2/3}$, implying that only elastic deformation is involved in the friction phenomenon. Bowden and Tabor (1950) and Maurer (1965) proposed to consider coefficient of friction as a function of normal load. Maurer (1965) suggested an empirical equation.

$$\tau = \mu_o \sigma^m \qquad \ldots.2.2.2$$

Where μ_o and m are constants obtained through observations over wide range of normal loads. Jaeger (1959) revised Coulomb's empirical work and advocated a linear equation for failure of a joint under shear.

$$\tau = S_o + \mu\sigma \qquad \ldots.2.2.3$$

Where S_o and μ are constants. This equation has been recognized as principal plank to further the understanding of friction phenomenon in jointed rocks.

2.3.0. STRENGTH OF INTACT AND JOINTED ROCKS

2.3.1. Strength of intact rocks

A great deal of work in the area of rock strength is from the classical theories (Coulomb, Mohr, Griffith etc.) with modification for various aspects. The following are the major attempts in this direction.

(i) Coulomb (1776) postulated that the shear stress tending to cause failure is resisted by the cohesion of the material plus a constant times the normal stress across the

plane of failure. It is expressed as

$$\tau = c + \sigma \tan \phi_{\mu} \qquad \ldots.2.3.1$$

(ii) Mohr (1900) conceptulized that, failure occurs by yielding and fracture. He assumes slippage as a mode of failure and provides a functional relationship as:

$$\tau = f (\sigma) \qquad \ldots.2.3.2$$

Graphically it is termed as Mohr rupture envelope which represents the locus of all points and defines the limiting values of both components of stress in the slip plane subject to different states of stress.

(iii) Griffith (1921) hypothesized that the failure is caused due to stress concentrations at the tips of minute cracks encased in the material. The failure is initiated when the maximum stress near the tip of most favourably oriented crack reaches a critical value. It is expressed as:

$$(\sigma_1 - \sigma_3)^2 = - 8 T_o (\sigma_1 + \sigma_3) \qquad \ldots.2.3.3$$

(iv) Weibull (1939) weakest link theory is a statistical theory for failure of general solids. His theory works out the distribution of strength of general solid within a body and also work out the probability that the solid would fail under a given stress. The vital point of the theory is its capability to predict the size effect.

(v) Mc Clintock and Walsh (1962) and Brace (1969 b) modified Griffith's theory by assuming that in compression Griffith's crack closes and a frictional force develops across the crack surface. Failure occurs when

$$\mu(\sigma_1+\sigma_3-2\sigma_c) + (\sigma_1-\sigma_3) (1+\mu^2)^{\frac{1}{2}} = 4 T_o \left[\frac{(1-\sigma_c)}{T_o} \right]^{\frac{1}{2}} \qquad \ldots.2.3.4$$

Brace pointed out that σ_c is small and can be neglected. Hence the equation 2.3.4 becomes

$$\mu(\sigma_1+\sigma_3) + (\sigma_1-\sigma_3)\ (1+\mu^2)^{\frac{1}{2}} = 4\ T_o \qquad \ldots.2.3.5$$

(vi) Murrell (1963) extended Griffith theory in three diamensions. It provides simple criterion for studying the effects of polyaxial stresses.

For triaxial test $\sigma_1 > \sigma_2 = \sigma_3$, it is

$$(\sigma_1-\sigma_3)^2 = 12\ T_o\ (\sigma_1+2\sigma_3) \qquad \ldots.2.3.6$$

Which is a parabola, whose slope when $\sigma_3 = 0$ is

$(d\sigma_1/d\sigma_3) = 4.$

For biaxial stress it is

$$\sigma_1^{\ 2}-\sigma_1\sigma_2 + \sigma_2^{\ 2} = 12\ T_o\ (\sigma_1+\sigma_2) \qquad \ldots.2.3.7$$

which is an ellipse, whose slope when $\sigma_2 = 0$ is

$(d\sigma_1/d\sigma_2) = 2.$

It intersects the line $\sigma_1=\sigma_2$ when $\sigma_2 = 24\ T_o$

If $\sigma_2 = \frac{1}{2}(\sigma_1+\sigma_3)$, the equation becomes

$$(\sigma_1-\sigma_3)^2 = 24\ T_o\ (\sigma_1+\sigma_3) \qquad \ldots.2.3.8$$

(vii) Wiebols and Cook (1968) using the strain energy theory suggested that the process of failure may be controlled by total amount of strain energy stored by the deformed specimen and fracture occurs when strain energy reaches a maximum value. The strain energy stored within the material prior to failure is computed from elastic deformation and more specifically from the shear distortion of closed micro-cracks. The total distortion energy W for large number of cracks will be the sum of all the shear energy. It is expressed as

$$W = K \int w(n\lambda)\ N(n\lambda)\ dn\ d\lambda \qquad \ldots.2.3.9$$

Where K is the constant whose value depends upon the elastic constants of surrounding materials. η and λ are orientation parameters of azimuth and latitudes of cracks respectively.

2.3.2. Strength of jointed rocks

A number of research contributions in the ares of strength of jointed rocks have been made by various workers. Most notable contributions among these are briefly described below:

(i) Newland and Alley (1957) indicated that shear is not an intrinsic property but depends upon the average angle of deviation of particle displacement from the direction of the applied stress.

(ii) Patton (1966) studied the influence of asperities and the phenomenon of interlocking on the failure enevelopes. His results from specimens of Kaoline and plaster mixes with different angles of inclination of asperities indicate the failure enevelopes as depicted in Fig.2.1. Figure 2.2 gives the influence of increasing number of asperities on shear strength. Figure 2.3 represents the results of investigations on two series of specimens with identical surface configuration but different internal strengths.

(iii) Einstein, Bruhn and Hirschfeld (1970) explained the influence of asperities and phenomenon of interlocking in rock friction. According to them the two surfaces may not be in plane contact but may be interlocking where certain portions are in tip to tip contact (Fig.2.4) but major portion of this is staggered. This interlocking influences the relationship between the shear force and the normal force.

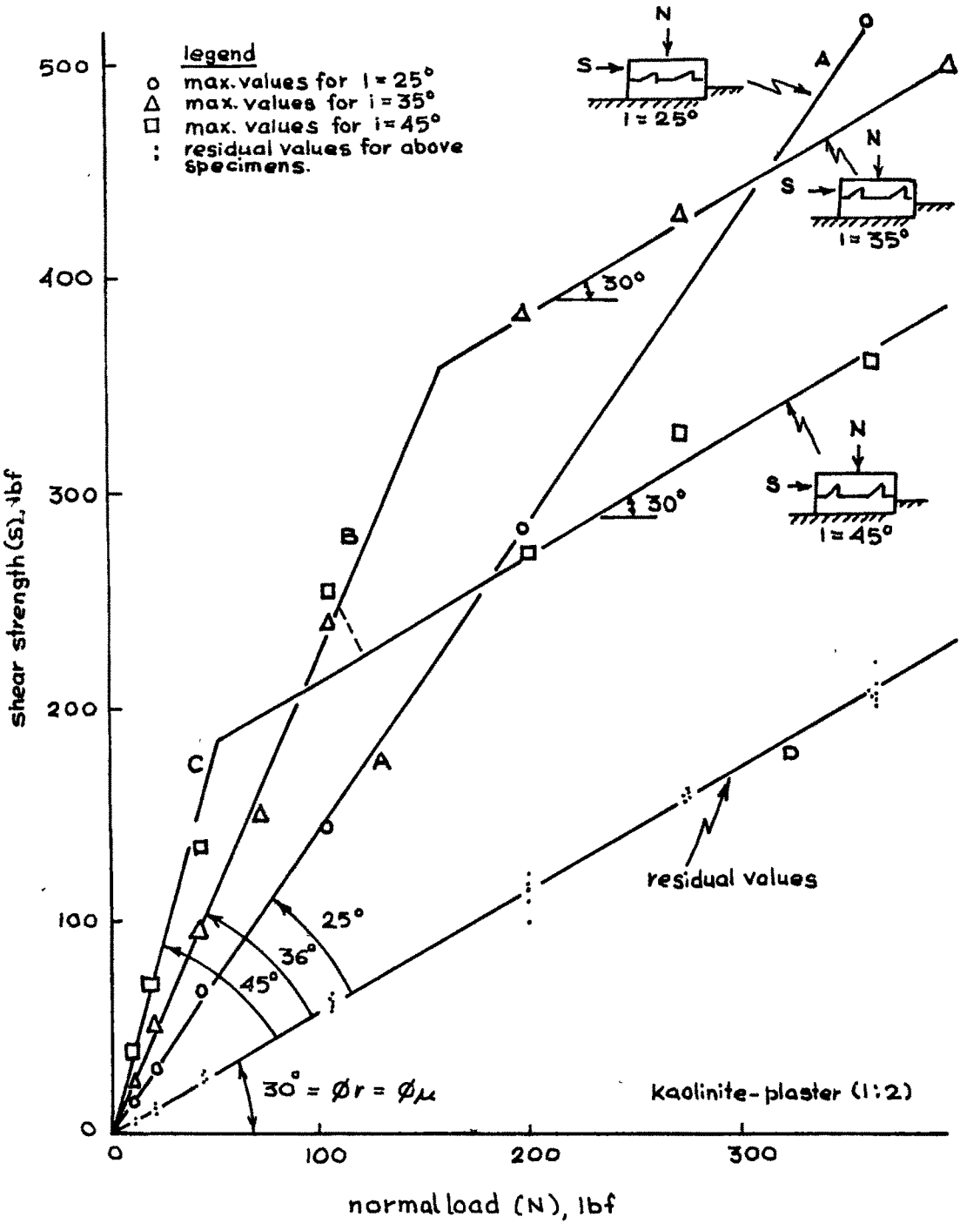

FIG. 2·1 FAILURE ENVELOPES FOR SPECIMENS WITH DIFFERENT INCLINATIONS OF TEETH

(after PATTON, 1966a)

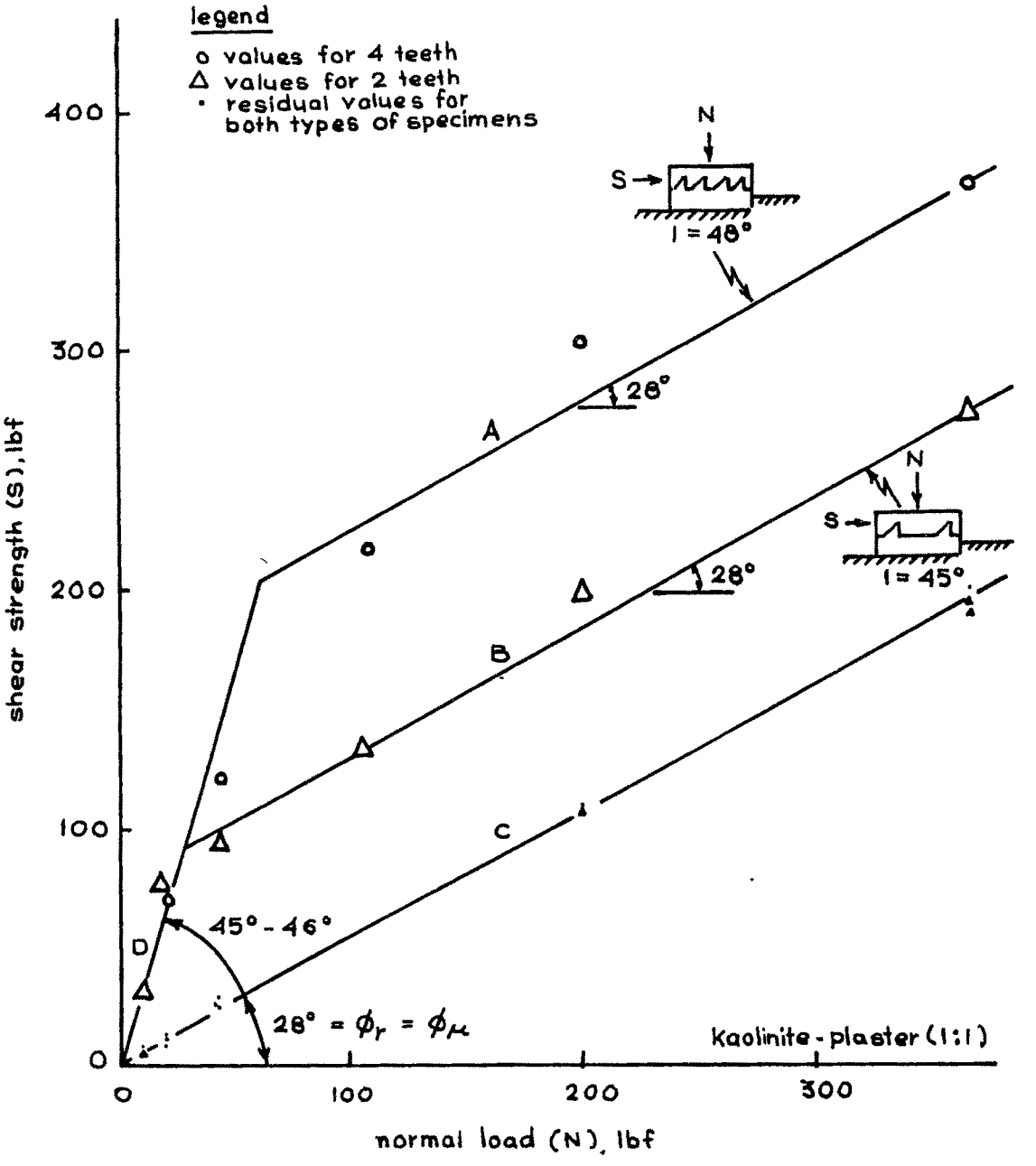

FIG. 2·2 FAILURE ENVELOPES FOR SPECIMENS FOR DIFFERENT NUMBER OF TEETH (after PATTON, 1966 a)

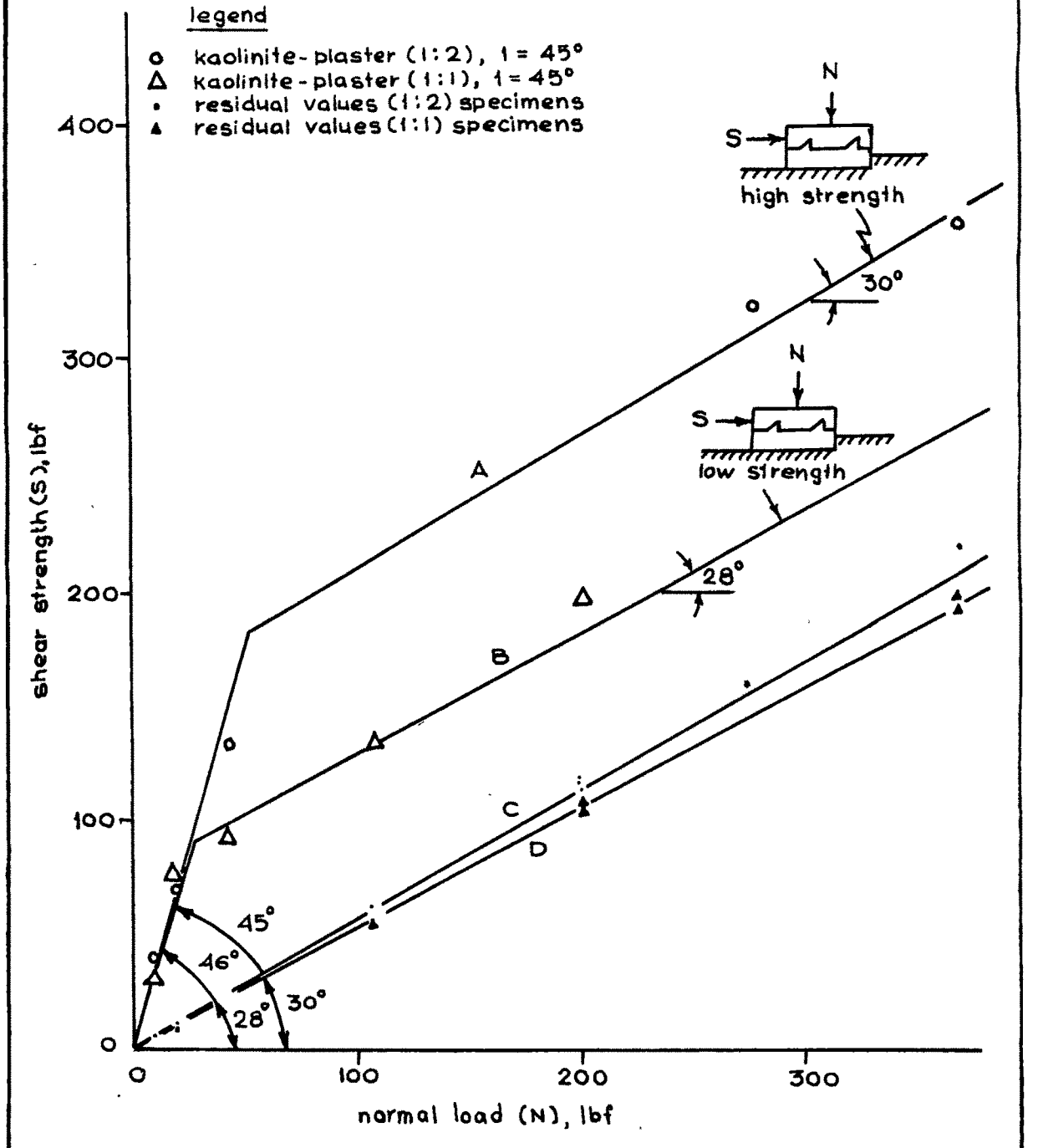

FIG. 2·3 FAILURE ENVELOPES OF SPECIMENS WITH DIFFERENT INTERNAL STRENGTHS (after PATTON, 1966 a).

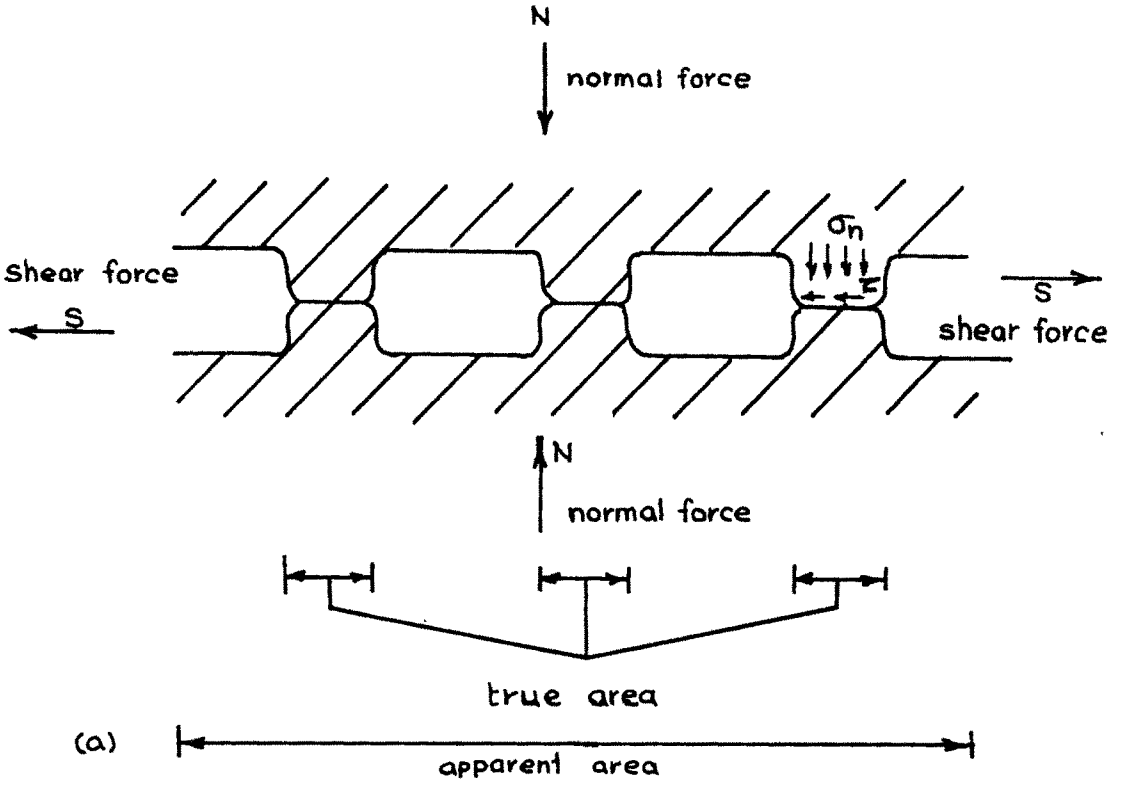

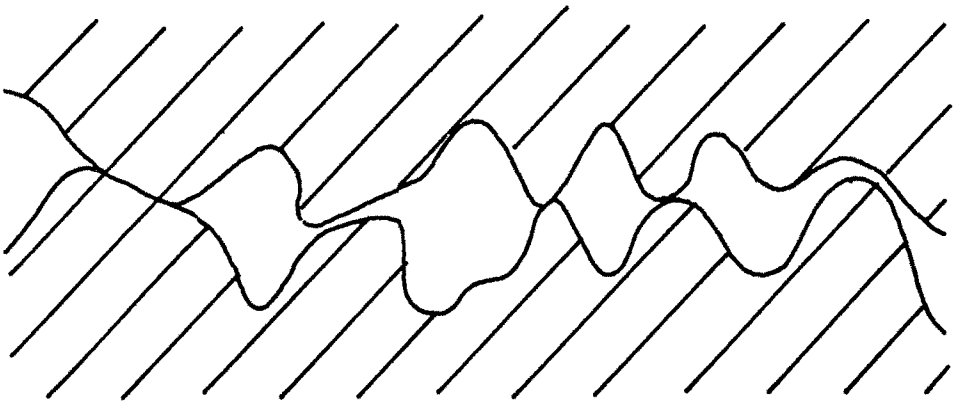

(b)

FIG. 2·4 (a) CONTACT OF ASPERITIES
(b) INTERLOCKING OF ASPERITIES
(after EISTEN, BRUHN AND HIRSCHFELD, 1970)

At small to medium values of normal force the asperities slide over each other and shearing resistance can be expressed as:

$$S = N \tan(\phi_\mu + i) \quad \ldots.2.3.10$$

where S = shear force

N = normal force

ϕ_μ = angle of frictional sliding resistance along plane surface

i = inclination of asperities with the horizontal along the movement

When asperities rides upto a certain level the stresses in asperities will reach the strength of asperities then the asperities will shear off.(Fig.2.5) At this stage the relation will be

$$S = K + N \tan \phi_r \quad \ldots.2.3.11$$

where ϕ_r = angle of residual shearing resistance of material

K = constant (intercept of S-N curve)

The above equations are based on the assumption that the shearing takes place in conformation with the geometry of the asperities and with full degree of interlocking. However, these assumption can not hold good in actual conditions.(Fig. 2.6)

(iv) Corthouts (1966) simulated the process of dilatancy and shearing of asperities in the finite element programme, using two asperities which are at 45° inclined to the horizontal and also symmetrical. According to computation of transverse and normal external loading the tensile stresses

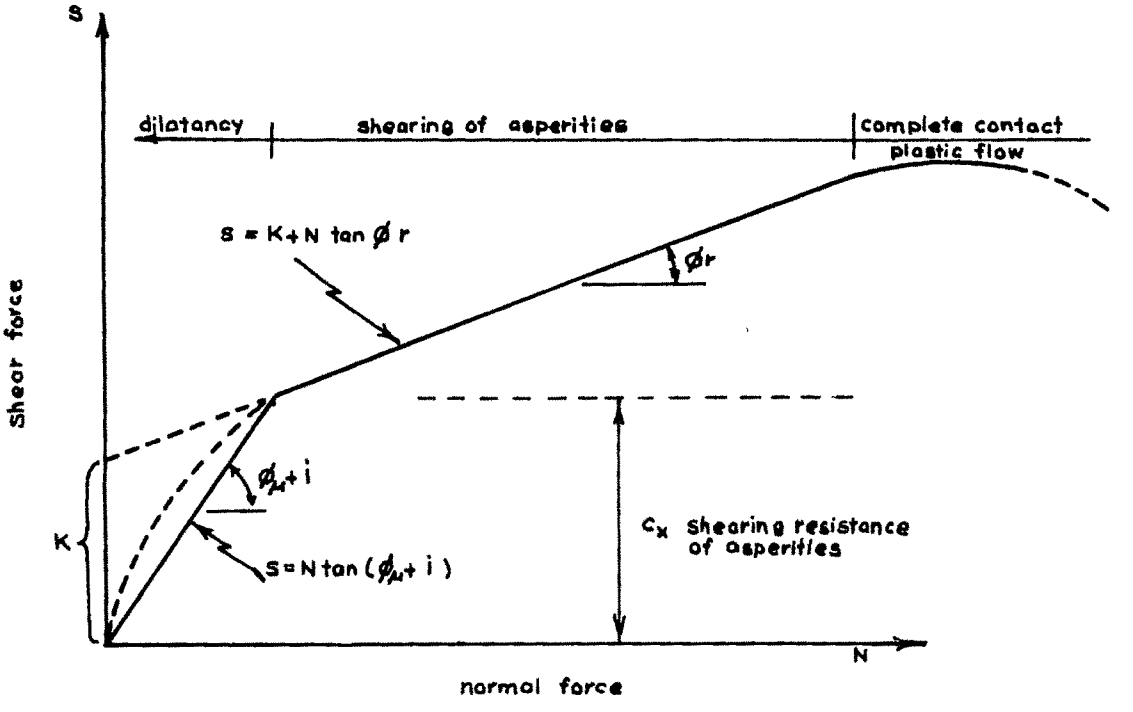

FIG. 2·5 DILATANCY OF SPECIMEN AND SHEARING OF ASPERITIES IN TYPICAL MOHR'S ENVELOPE.

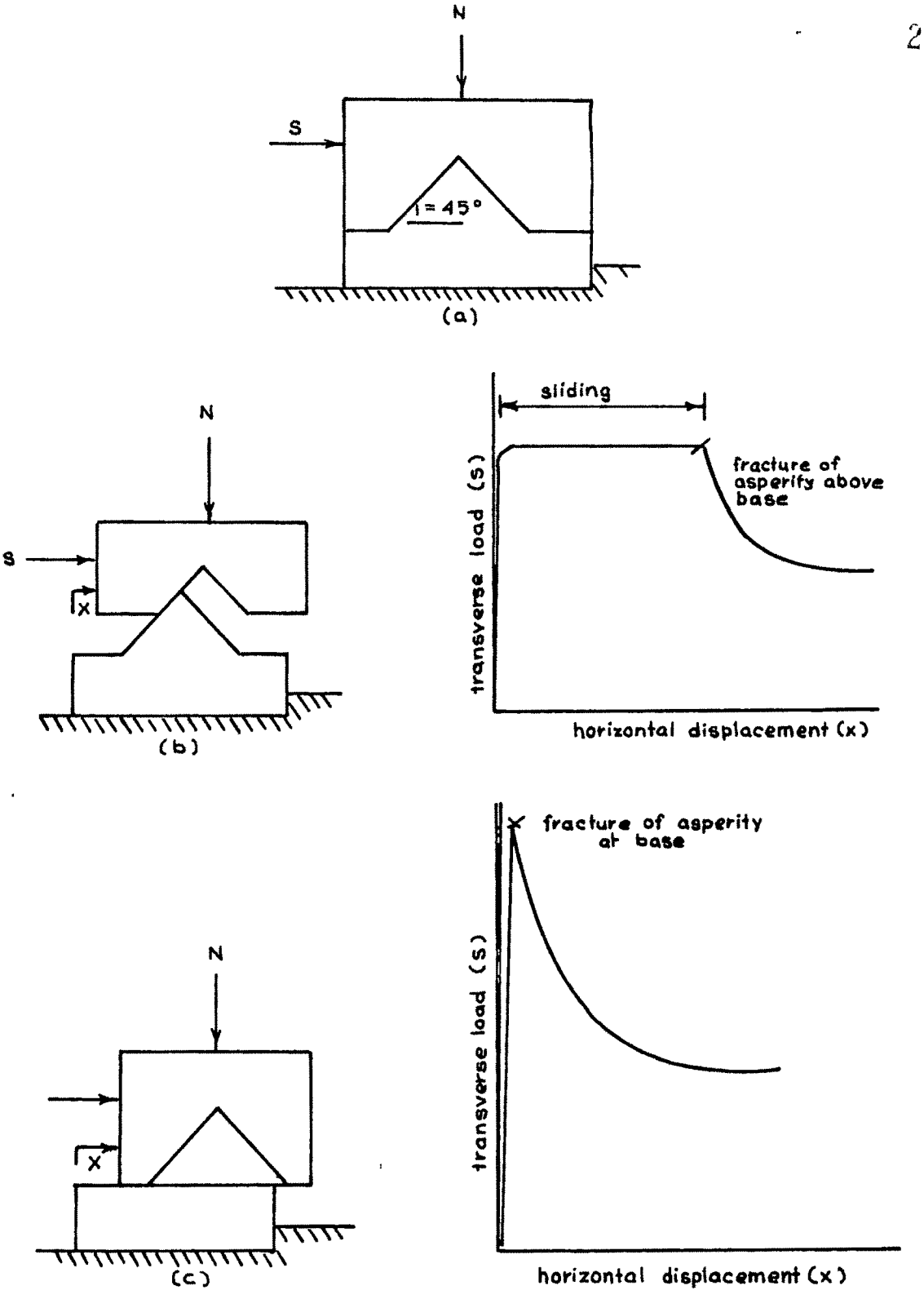

FIG.2·6 THE MECHANISM OF DILATANCY & SHEARING OF THE ASPERITY WITH THE CORRESPONDING LOAD DISPLACEMENT CURVES.

a) Initial stage (before displacement)
b) Displacement with dilatancy & shear at a larger stage.
c) Shearing without dilatancy.

(after EINSTEIN, BRUHN and HIRSCHFELD, 1970)

are greater than the tensile strength. He further obtained bilinear Mohr's envelope from static and finite element analysis as shown in (Fig.2.7 a,b).

(v) Rowe, Barden and Lee (1964) developed an expression for shear force for the case of direct shear test. According to them the shear force may be divided into three components:

$$S = S_1 + S_2 + S_3 \qquad \ldots.2.3.12$$

where, S_1 = shear force component due to external work done in dilating against the external force N.

S_2 = shear component due to additional internal work done in friction due to dilatancy

S_3 = shear force component due to work done in values of these internal friction if the specimen did not change in volume in shear

The components can be worked out from the first principles. (Fig. 2.8) Accordingly,

$$S_1 = N \tan i = N \dot{V} \qquad \ldots.2.3.13$$

where $\dot{V}$ = rate of dilation at failure i.e. $\frac{dy}{dx}$

$$S_2 = S \tan i \tan \phi_\mu = S \dot{V} \tan \phi_\mu \qquad \ldots.2.3.14$$

when there is no dilation,

$$S_3 = N \tan \phi_\mu \qquad \ldots.2.3.15$$

Thus,

$$S = N \tan i + S \tan i \tan \phi_\mu + N \tan \phi_\mu \qquad \ldots2.3.16$$

i.e. $$S/N = \tan (\phi_\mu + i) \qquad \ldots.2.3.17$$

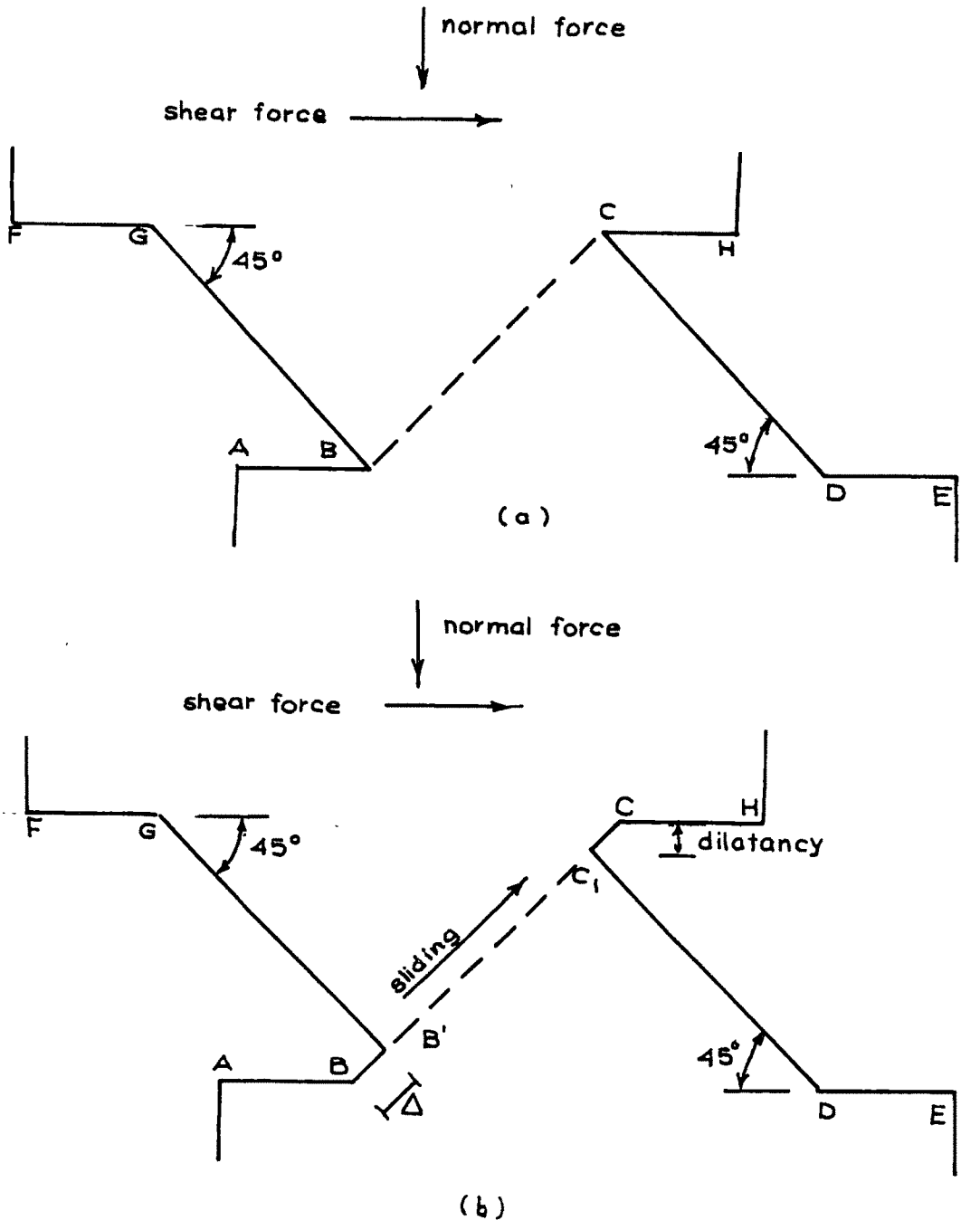

FIG 2.7a ANALYTICAL MODEL USED BY CORTHOUTS (1966) FOR FINITE ELEMENT ANALYSIS THE MODEL CONSISTS OF TWO ASPERITIES SUBJECTED TO NORMAL & SHEAR FORCES.

a) INITIAL SITUATION. b) FIRST STEP AFTER SLIDING.

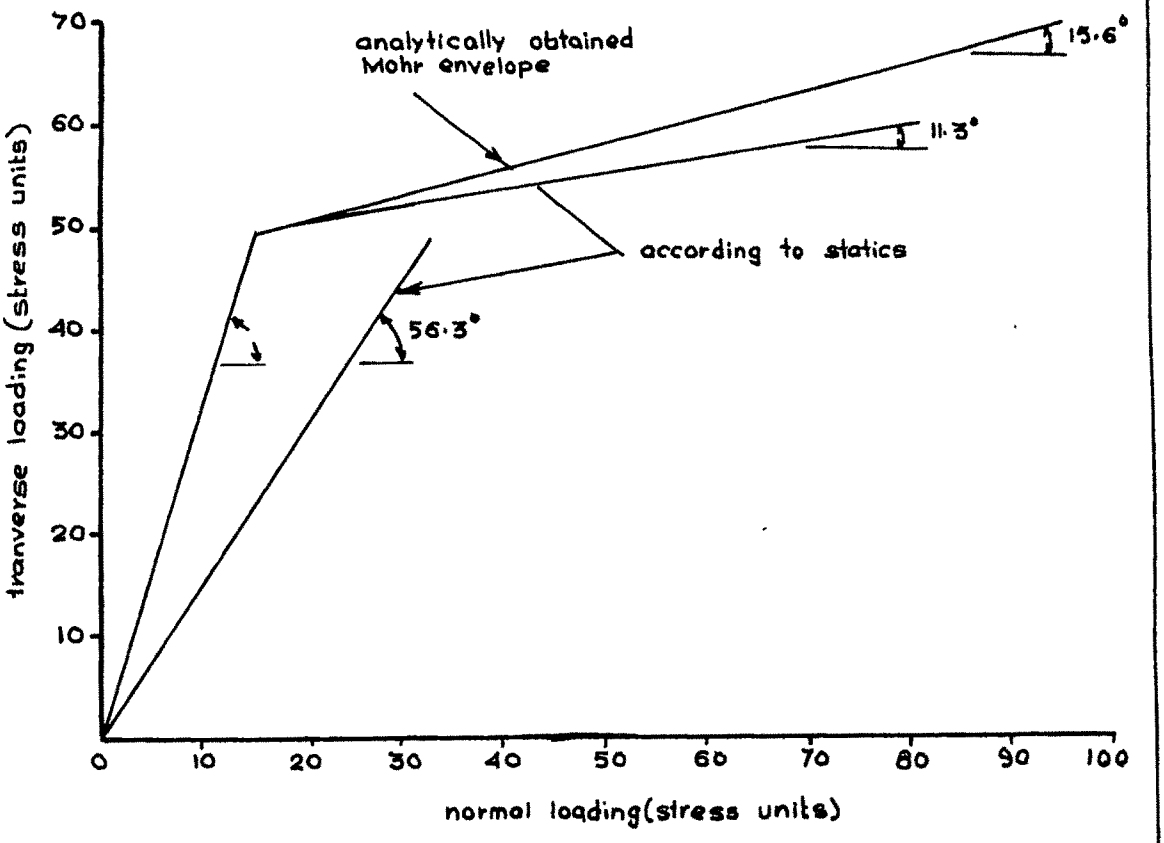

FIG. 2·7 b COMPARISON BETWEEN THE MOHRS ENVELOPES FOR TWO ASPERITIES OBTAINED BY CORTHOUTS (1966) FOR THE CASE SHOWN IN FIG. 2·7 a
($\phi_\mu = 11{\cdot}3^\circ, \sigma_t = 3090$ lbf/in)

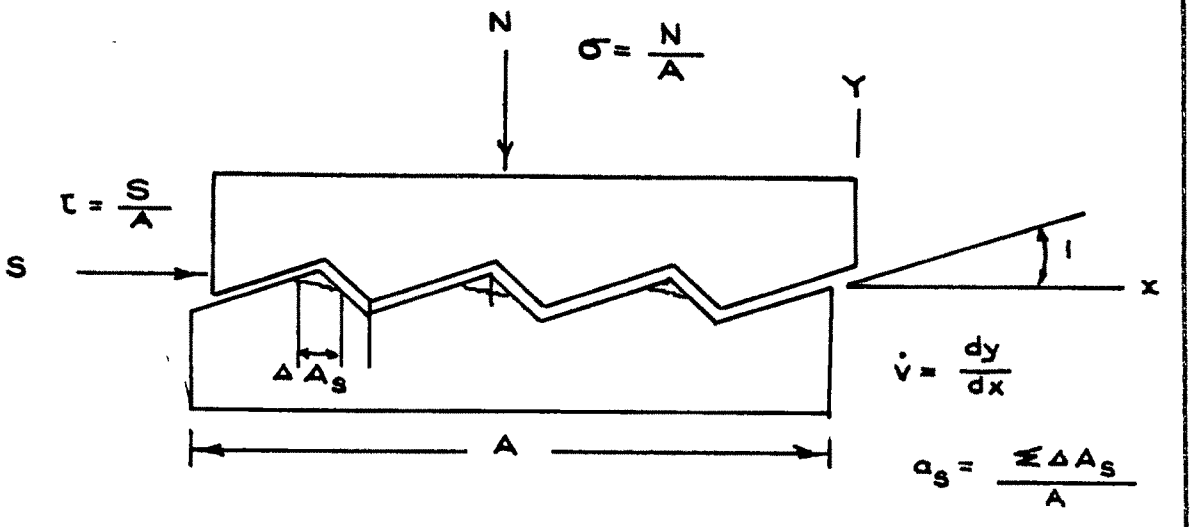

FIG. 2-8 DEFINITION OF THE DILATION RATE $\dot{v}$ AND THE SHEAR AREA RATIO OF a_s.

(vi) Ladanyi and Archambault (1969) suggested a fourth component to the above work for an irregular rock surface due to the shearing of the teeth

$$S_4 = A\,K + N \tan \phi_o \qquad \ldots.2.3.18$$

where A = total projected area of the teeth at the plane of shear.

K and ϕ_o = Coulomb shear strength parameters.

This equation for S_4 can be written on the assumption that all the teeth are sheared off at the base.

For real case the shearing along an irregular surface consists of simultaneous occurance of two modes of failure i.e. sliding and shearing.

The total shear force can be written by

$$S = (S_1+S_2+S_3)(1-a_s) + S_4 a_s \qquad \ldots.2.3.19$$

where $a_s = A_s/A$ = shear area ratio.

Thus for

$$\tau = S/A = \frac{\sigma_n(1-a_s)(\dot{V}+\tan\phi_\mu)+(\sigma_n \tan\phi_o+K)a_s}{1-(1-a_s)\dot{V}\tan\phi_\mu} \qquad \ldots.2.3.20$$

when $\dot{V} = 0$, the expression 2.3.20 becomes

$$= \sigma_n(1-a_s)\tan\phi_\mu + a_s(\sigma_n \tan\phi_o + K) \qquad \ldots.2.3.21$$

In view of observed curvature of the Mohr's envelope, Fairhurst (1964) proposed a parabolic law:

$$= \sigma_c\left(\frac{m-1}{n}\right)\left(1+\frac{n\sigma_n}{\sigma_c}\right)^{\frac{1}{2}} \qquad \ldots.2.3.22$$

where $n = \dfrac{\sigma_c}{-\sigma_t}$

σ_c = uniaxial compressive strength of solid rock

σ_t = uniaxial tensile strength of solid rock and

$$m = (n+1)^{\frac{1}{2}}$$

Substituting 2.3.22 in 2.3.20 it yields:

$$= \frac{\sigma_n(1-a_s)(\dot{V}+\tan \phi_u) + a_s\sigma_c\left(\frac{m-1}{n}\right)\left(1+n\frac{\sigma_n}{\sigma_c}\right)^{\frac{1}{2}}}{1-(1-a_s)\,\dot{V}\tan \phi_\mu} \quad \ldots.2.3.23$$

They found good corelation between these equations and shear strength of models composed of small elements in a biaxial shear box. (Fig. 2.9)

(vii) Barton (1971,1973) recommended for practical field applications, an empirical relationship between shear strength and effective normal stress expressed by an equation:

$$\tau = \sigma' \tan\left[\phi_b + JRC \log_{10}(JCS/\sigma')\right] \quad \ldots.2.3.24$$

where ϕ_b = basic friction angle of smooth planar discontinuties in the rock.

JRC = joint roughness coefficient which ranges from 5 for smooth surface to 20 for rough undulating surface.

JCS = joint wall compressive strength which for clean unweathered discontinuties, equals the uniaxial compressive strength of intact rock.

Similar expressions have been proposed by Krsmanovic (1967) Martin and Miller (1974) and Hencher and Richards (1982).

(viii) Hoek and Brown (1980) proposed an approximate method for estimating strength of jointed rock masses. It consists in assigning the values to the empirical constants from description of rock mass and to find unconfined strength of intact rock for construction of modified Mohr's failure enevolope to estimate the strength of jointed rock.(Fig.2.10)

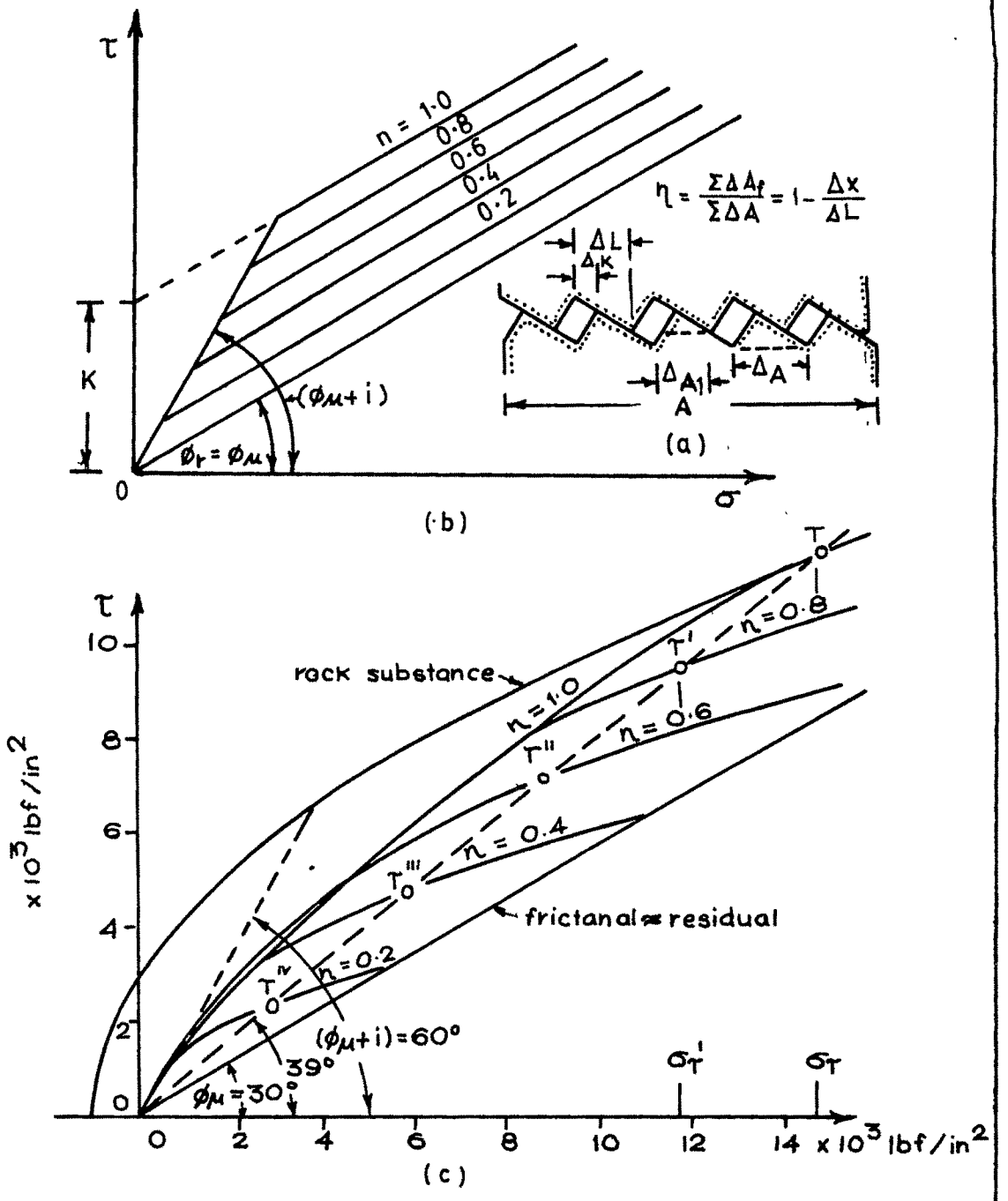

FIG. 2-9 INFLUENCE OF DECREASING DEGREE OF INTERLOCKING OF ASPERITIES ON THE SHEAR STRENGTH ALONG IRREGULAR ROCK SURFACES.
(b) RESULTS ACCORDING TO BILINEAR MODEL
(c) RESULTS ACCORDING TO EQUATION
(after LADANYI and ARCHAMBAULT, 1969).

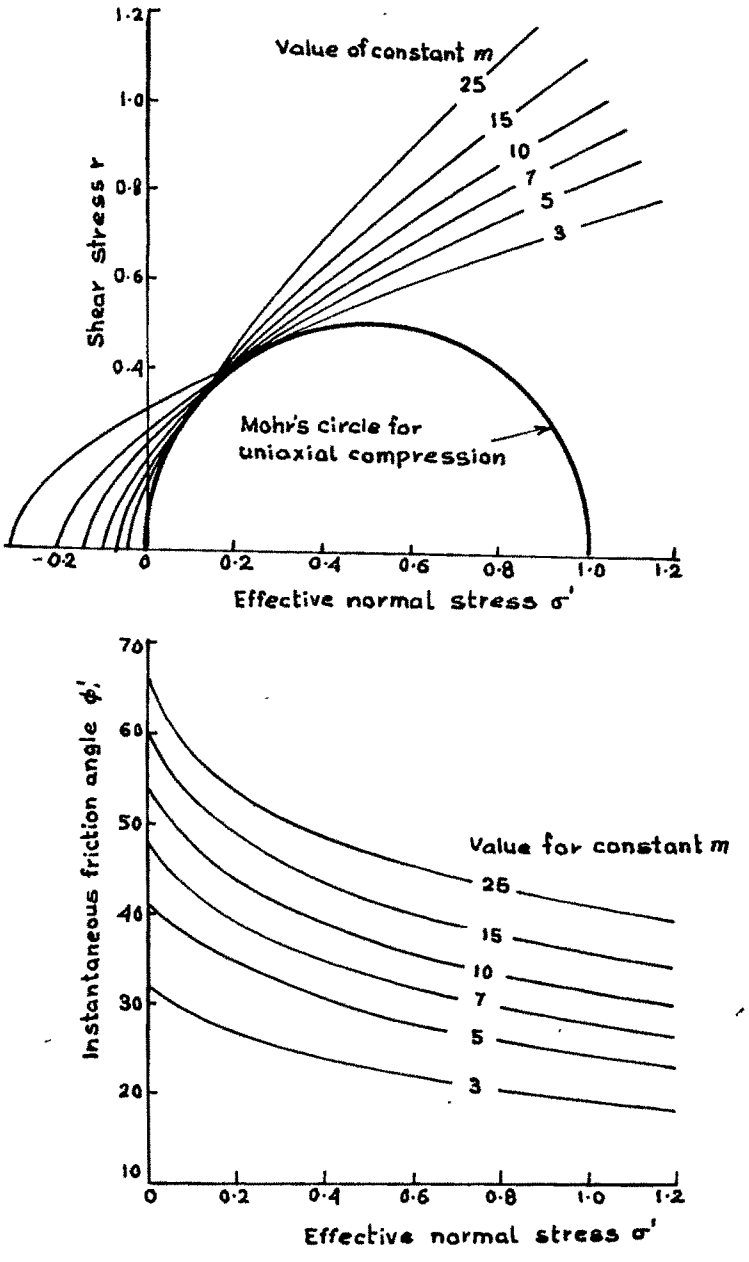

FIG.2·10 INFLUENCE OF THE VALUE OF THE CONSTANT m ON THE SHAPE OF THE MOHR FAILURE ENVELOPE AND ON THE INSTANTANEOUS FRICTION ANGLE AT DIFFERENT EFFECTIVE NORMAL STRESS LEVELS
(after HOEK and BROWN, 1980)

The empirical relationship between principal major and minor stresses at failure is

$$\sigma_1 = \sigma_3 + \sqrt{(m\,\sigma_c\sigma_3 + S\,\sigma_c^2)} \qquad \ldots.2.3.25$$

where σ_1 = major principal effective stress at failure

σ_3 = minor principal effective stress at failure or confining pressure in case of conventional triaxial test.

σ_c = uniaxial compressive strength of intact rock material.

m = empirical constants which ranges from 0.001 for highly disturbed rock mass to about 25 for hard intact rock.

S = empirical constant, zero for jointed rock mass to one for intact rock material.

2.4.0. SLIDING BEHAVIOUR OF ROCK JOINTS

2.4.1. Types of joints

The term rock joints is used to describe the mechanical discontinuities of geological origin that intersect near surface of rock masses. In very general terms primarily there are two types of natural joints (a) tension joints and (b) shear joints. In contrast to tension joints shear joints will often be markedly planar. Joints planar in nature are generally associated with plastic deformation as opposed to brittle deformation. In addition to these naturally occuring joints there are artificial joints produced as a result of fracturing of intact rocks and a wide variety of artificial planar sawn surfaces. For purposes of

failure analysis of joints possible modes of failure are identified as (a) translation (b) toppling and (c) circular. Research studies are directed towards the determination of shear strength of planar and nonplanar joints.

2.4.2 Sliding along a single joint system

On the assumption that the simple two diamentional criterion of slip along the plane is valid, the single joint system has been analysed by Jaeger and Cook (1969 a). For a triaxial conditions of $\sigma_1 > \sigma_2 = \sigma_3$ there is a plane of weakness whose normal makes an angle α with the greatest principal stress σ_1 (Fig. 2.11 a). The criterion for slip in the plane is

$$\tau = S_o + \mu\sigma \qquad \ldots.2.4.1$$

where σ and τ are the normal and shear stresses across the plane.

Now, σ and τ are given by

$$\sigma = \tfrac{1}{2}(\sigma_1+\sigma_2) + \tfrac{1}{2}(\sigma_1-\sigma_2) \text{ Cos } 2\alpha \qquad \ldots.2.4.2$$

$$\tau = -\tfrac{1}{2}(\sigma_1-\sigma_2) \text{ Sin } 2\alpha \qquad \ldots.2.4.3$$

These may be put in the alternative form

$$\sigma = \sigma_m + \tau_m \text{ Cos } 2\alpha \qquad \ldots.2.4.4$$

$$\tau = -\tau_m \text{ Sin } 2\alpha \qquad \ldots.2.4.5$$

where σ_m is the mean stress and τ_m the maximum shear stress so that

$$\sigma_m = \tfrac{1}{2}(\sigma_1+\sigma_2) \quad \text{and } \tau_m = \tfrac{1}{2}(\sigma_1-\sigma_2) \qquad \ldots.2.4.6$$

putting $\mu = \tan \phi$ $\ldots.2.4.7$

where ϕ is the angle of friction and using equations 2.4.4 and 2.4.5 in equation 2.4.1.

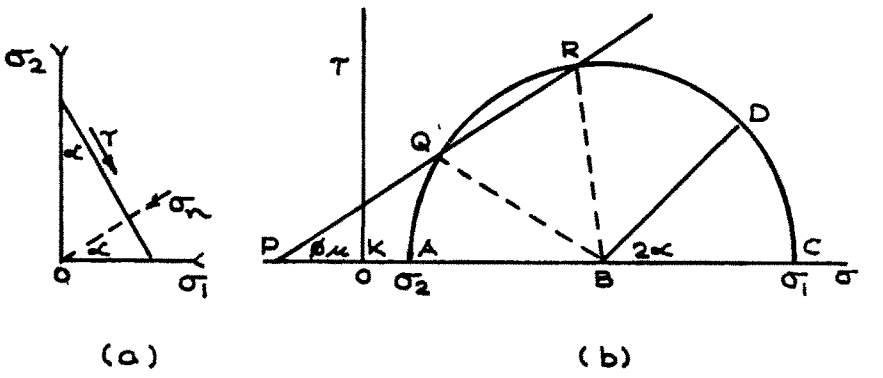

FIG. 2-11 SLIDING ON A PLANE OF WEAKNESS: TWO-DIMENSIONAL THEORY.

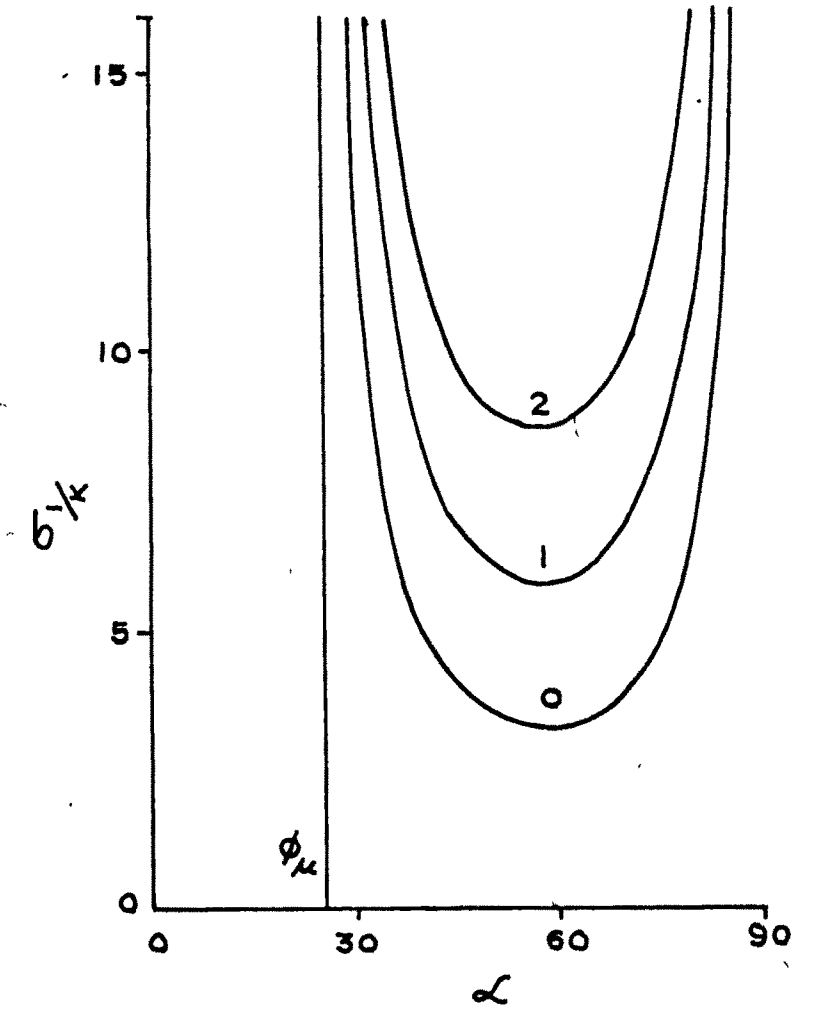

FIG. 2-12 THE VARIATION OF σ_1 WITH α FOR SLIDING ON A PLANE OF WEAKNESS WITH $\mu = 0.5$. NUMBERS ON THE CURVES ARE THE VALUES OF σ_2/K.
(after JAEGER and COOK, 1969 a).

$$\tau_m \left(\sin 2\alpha - \tan \phi \cos 2\alpha \right) = S_o + \sigma_m \tan \phi \quad \ldots.2.4.8$$

$$\tau_m = (\sigma_m + S_o \cot \phi) \tan \delta \quad \ldots.2.4.9$$

where $\tan \delta = \sin \phi \operatorname{cosec} (2\alpha - \phi)$

Alternatively, the criterion of slip can be written as ;

$$(\sigma_1 - \sigma_2) = \frac{2K + 2\mu \sigma_2}{(1 - \mu \cot \alpha) \sin 2\alpha} \quad \ldots.2.4.10$$

and if $n = \sigma_2/\sigma_1$ then

$$\sigma_1 = \frac{2K \cot \phi}{(1-n) \sin (2\alpha - \phi) - (1+n)} \quad \ldots.2.4.11$$

The above equations 2.4.1, 2.4.8, 2.4.9, 2.4.10 and 2.4.11 are different ways of expressing the criterion of failure. The stress difference necessary to cause failure varies with α for fixed σ_2 and μ. As $\alpha \to \pi/2$ i.e. plane moves towards the direction of σ_1, $(\sigma_1 - \sigma_2) \to \infty$.
Also when $\alpha \to \tan^{-1}\mu = \phi$ the value of $(\sigma_1 - \sigma_2) \to \infty$. This means that failure is possible only when $\phi < \alpha < \pi/2$ and the minimum value of $(\sigma_1 - \sigma_2)$ can be given by

$$(\sigma_1 - \sigma_2) = 2(K + \mu\sigma_2) \left[(\mu^2+1)^{\frac{1}{2}} + \mu \right] \quad \ldots.2.4.12$$

The variation of σ_1 with α for the case of $\mu = 0.50$ is shown in figure 2.12. This is also clear in Mohr diagram figure 2.11 b. The criterion for failure is represented by the line P-Q-R inclined at an angle ϕ to the O-σ axis and making an intercept OP = -K Cot ϕ on this axis. The point D on Mohr circle with AC as diameter represents the normal and shear stresses. If D lies in either of the arcs A-Q or R-C, these stresses would not be sufficient to cause slip

but if it lies in the arc Q-R, then stresses would be sufficient to cause slip.

This theory is applicable for (i) the sliding across open joints where K is shear strength of joint (ii) sliding along filled joints where K is the shear strength of the filling material and μ coefficient of internal friction of the filling materials (iii) the anisotropic material with parallel planes of weakness.

When there is possibility of failure through the material in a plane which intersects the plane of weakness and if the inherent shear strength of the material is S_o and the coefficient of internal friction is μ_o as per Coulomb criterion concept $S_o > K$ and $\mu_o > \mu$, the situation can be represented by figure 2.13 a. As shown above failure is possible when $\phi_\mu < \alpha < \pi/2$, and the criterion of slip between these limits can be represented by equation 2.4.11 and rewritten as

$$\sigma_1 = \sigma_2 + \frac{2K + 2\mu\sigma_2}{(1-\mu \cot\alpha)(\sin 2\alpha)} \qquad \ldots.2.4.13$$

For a given value of σ_2, the minimum value of $\sigma_1 (\sigma_{min})$ occurs when $\tan 2\alpha = -1/\mu$

$$\sigma_{min} = \sigma_2 + 2(K+\mu\sigma_2)\left[(\mu^2+1)^{\frac{1}{2}} + \mu\right] \qquad \ldots.2.4.14$$

If the value of σ_2 is constant and σ_1 is increased to the plane represented by the line A-B figure 2.13 b, i.e. along the plane of weakness α but if it is possible to increase the stress conditions such that $\sigma_1 = \sigma_{max}$, then failure is possible along the plane represented by the line C-D figure 2.3 a, i.e. along the plane of weakness α_o. Since the

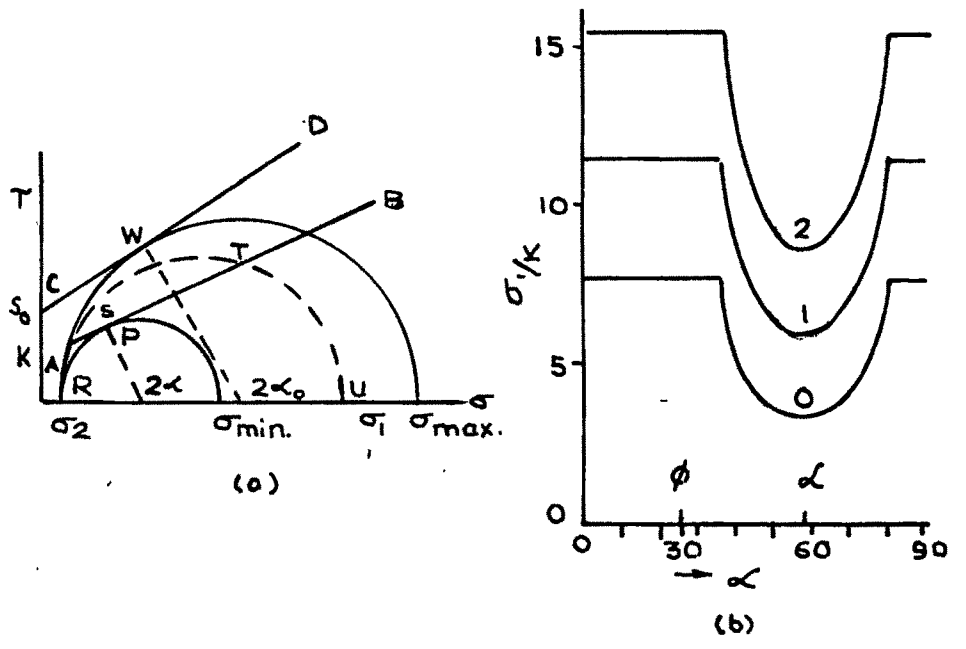

FIG·2·13 (a) FRACTURE IN AND ACROSS PARALLEL PLANES OF WEAKNESS IN A MATERIAL

(b) VARIATION OF σ_1 WITH α FOR THE CASE $\mu = 0{\cdot}5, \mu_0 = 0{\cdot}7$, $S_0 = 2K$. NUMBERS ON THE CURVES REFER TO THE RATIO (after JAEGER and COOK, 1969 a).

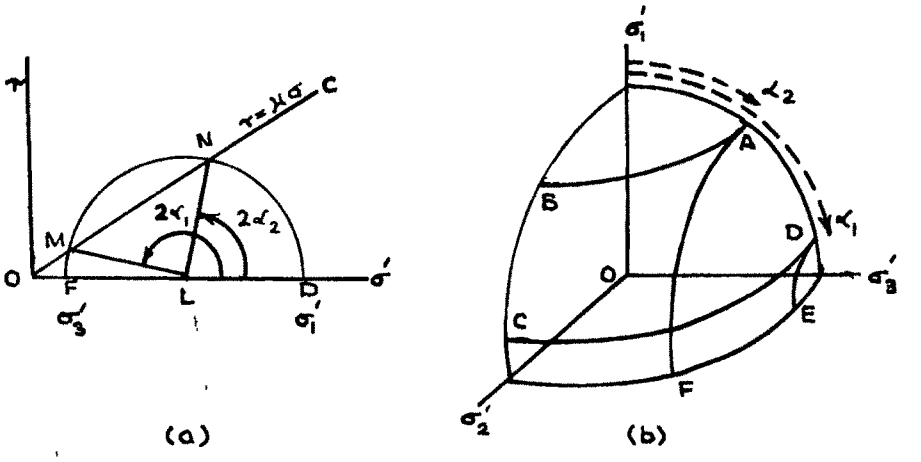

FIG. 2·14 (a) MOHR'S DIAGRAM FOR THE CASES $\sigma_2' = \sigma_3'$ OR $\sigma_2' = \sigma_1'$

(b) AN OCTANT OF SPHERE SHOWING THE REGION ABCD IN WHICH SLIDING IS POSSIBLE IF $\sigma_2' = \sigma_3'$ AND THE REGION ADEF IN WHICH SLIDING IS POSSIBLE WHEN $\sigma_1' = \sigma_2'$ (after JAEGER and COOK, 1969 a).

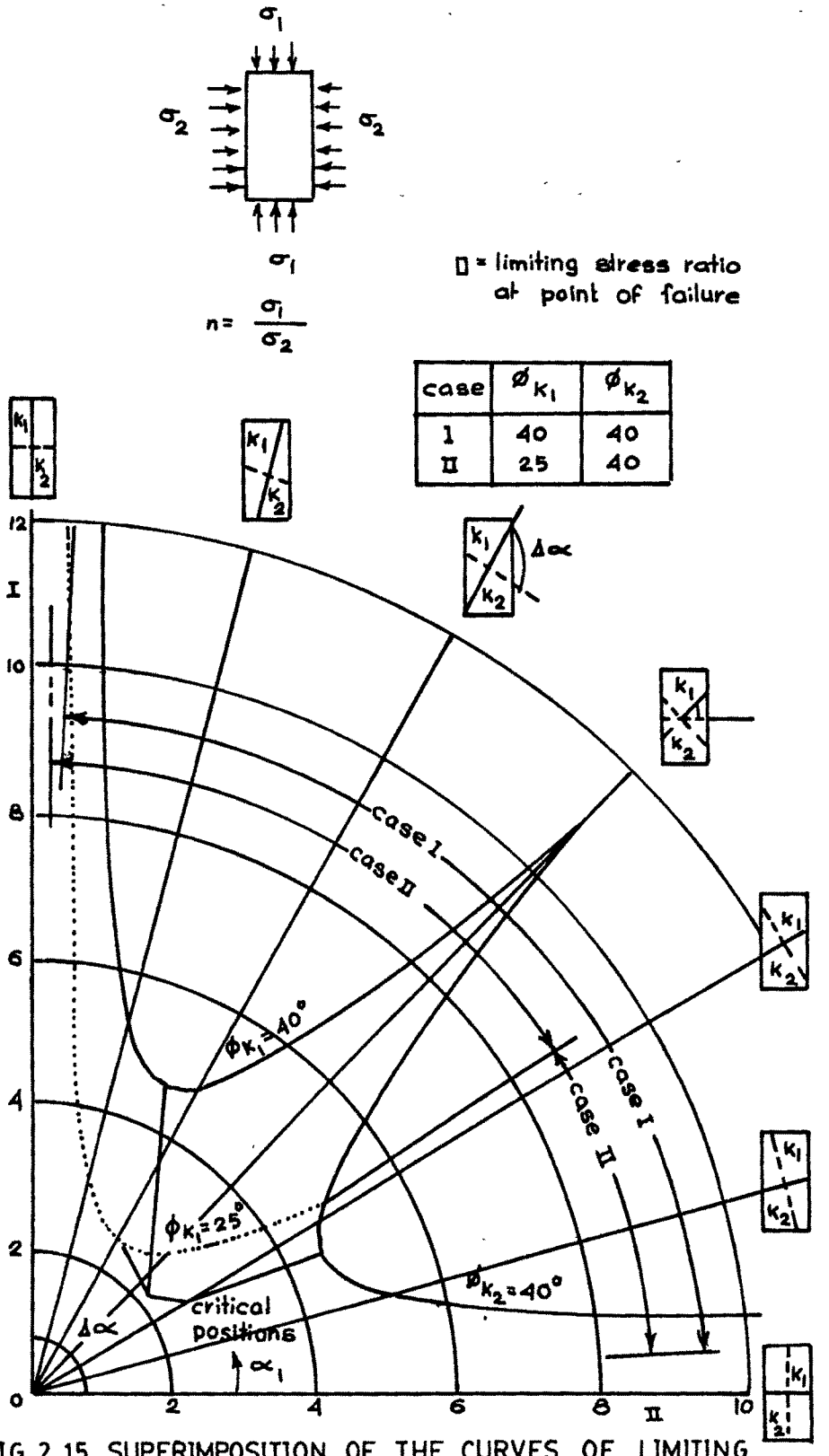

FIG 2 15 SUPERIMPOSITION OF THE CURVES OF LIMITING STRESS RATIO FOR TWO ORTHOGONAL JOINTS K1 & K2 FOR DIFFERENT VALUES OF THE FRICTION ANGLES (ϕ_{K_1} = 40°, 25° & ϕ_{K_2} = 40°)

CASE I REFERS TO $\chi_e = 1$; CASE II REFERS TO $\chi_e = 0.5$ WHERE χ_e = DEGREE OF CONTINUTY OF THE JOINT. (after JOHN, 1969).

line C-D represents the Mohr's envelop for solid material, the maximum value of σ_1 can then be represented by.

$$\sigma_{max} = \sigma_2 + 2(S_o + \mu_o \sigma_2)\left[(\mu_o^2 + 1)^{\frac{1}{2}} + \mu_o\right] \quad \ldots.2.4.15$$

The minimum and maximum values of σ_1 are given by the equations 2.4.14 and 2.4.15 when the angle of possible failure varies from α to α_o. The variation of σ_1 with α for a particular case is shown in figure 2.13 b.

2.4.3. Double or multiple joint system

The case of multipla joint system can be studied best by considering three dimensional case as represented by Mohr's diagram figure 2.14 a, b. The influence of two (or even more) joints occuring together can be clearly shown using the interpretation given in figure 2.15. In this it is possible to superimpose two joints or joint groups. Figure 2.15 shows two joint systems K_1 and K_2 placed at an angle of 90° to each other for different values of ϕ_μ plotted in polar coordinate system. Depending upon the angle of orientation of these joints with respect to the principal stress conditions the possibilities of sliding can be marked. (Fig.2.15)

2.5.0. FACTORS INFLUENCING FAILURE OF JOINTED ROCKS

2.5.1 Influence of roughness of the surface

Surface roughness is perhaps the most important factor which influences significantly the friction in jointed surfaces. A number of experimental studies have been conducted to evaluate the influence of surface roughness on the friction values. Following are the major findings of various research workers.

(i) Tschebotarioff and Welch (1948) found that the

friction coefficient of 0.106 for polished quartz mineral particles under dessicator ($CaCl_2$) condition rose to 0.37 for roughned particles.

(ii) Ripley and Lee (1961) observed that the sliding resistance friction angles corrected for dilation were higher for rough surfaces than ground surfaces in case of sand stone, silt stone and shale (Table 2.1)

TABLE 2.1

Sliding resistance friction angles obtained from plane and rough surfaces

(after Ripley and Lee, 1961)

	Plane surfaces (Series B) 2.3 in (58 mm) square		Natural rough surfaces (Series A) 6 in (150 mm) diameter			
			Corrected		Measured	
	Groung smooth	Sand-blast	lower	peak	lower	peak
Sandstone	25°	29°	27°	36°	40°	54°
Siltstone	25	31	32	34	43	47
				31*		45*
			21	24	26	34
Shale	26	27	24	35	26	35
			25	39	31	39

* Test not carried beyond peak value.

40

(iii) Einstein et al (1969) contradicting Ripley and Lee (1961) reported that residual sliding angle remains constant but apparent cohesion is greater for rougher surfaces.

(iv) Horn and Deere (1962) working on etched and polished surfaces found that etching of polished quartz substantially increases the friction value under saturated conditions (Fig. 2.16 and 2.17).

(v) Rae (1963) found that after certain amount of wear between lime stone slider and sand stone friction wheel the coefficient of friction fell considerably from 0.45 to 0.30.

(vi) Byerlee (1967 b) reported that the coefficient of friction of finely ground surface is lower than that for coarsely ground surfaces.

(vii) Hoskins, Jaeger and Rosengren (1968) observed that the coefficient of friction for rough surfaces of trachyte was 0.68 while for polished surfaces was 0.58.

(viii) Coulson (1970) indicated that the surface roughness effectively increases initial friction for many rock types viz. basalt, granite, sand stone, gneiss, dolomite, limestone, silt stone, shale.

(ix) Chappell (1975) Jaeger (1971) Rosengren(1968) working on rock joints using conventional shear box and conventional triaxial test observed that in all cases the rough surfaces gave higher value of friction coefficient.

It is probable that if influence of dilation and relative rotation are accounted the friction value is independent of nature of surface.

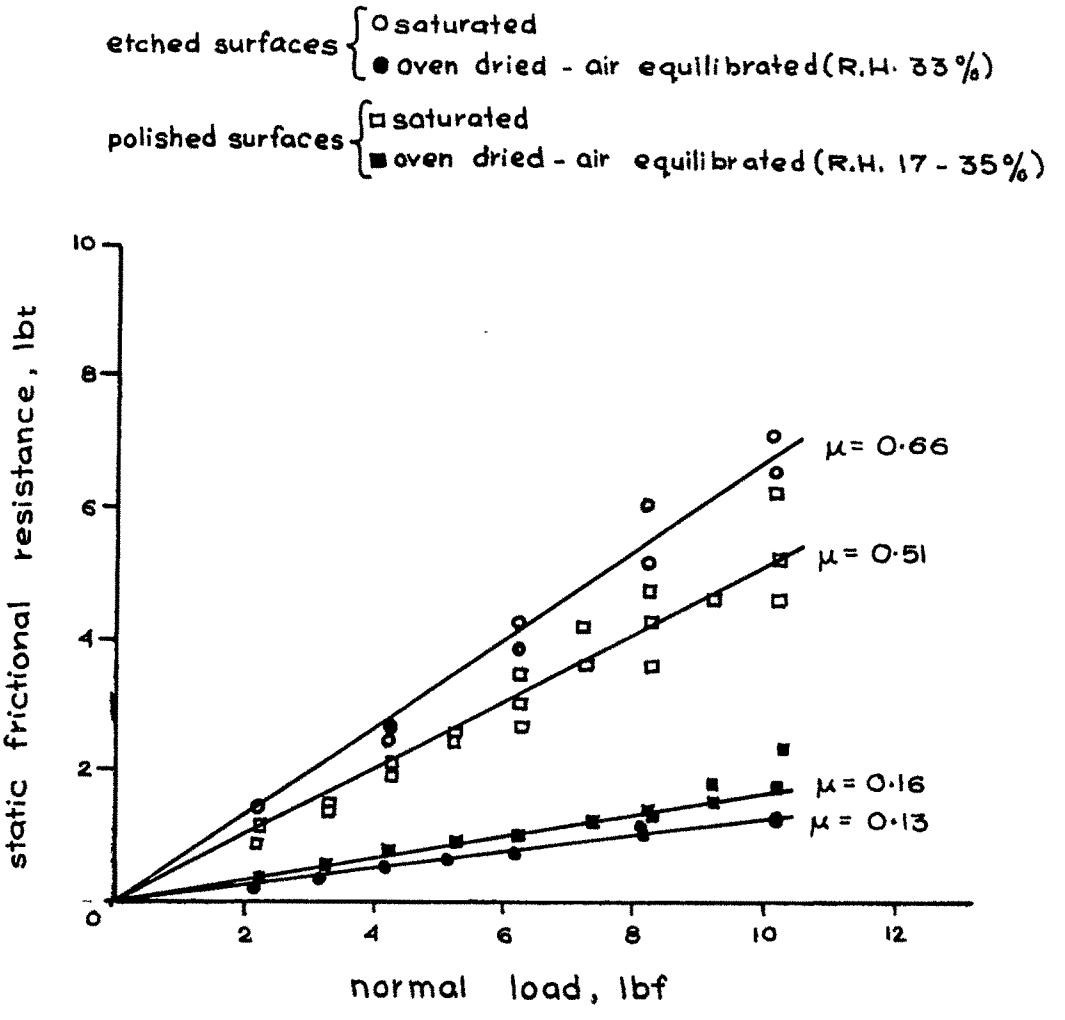

FIG. 2-16 THE EFFECT OF ETCHING ON THE STATIC FRICTIONAL CHARACTERISTICS OF POLISH SURFACES OF MILKY QUARTZ (WISCONSIN)
(after HORN and DEERE, 1962).

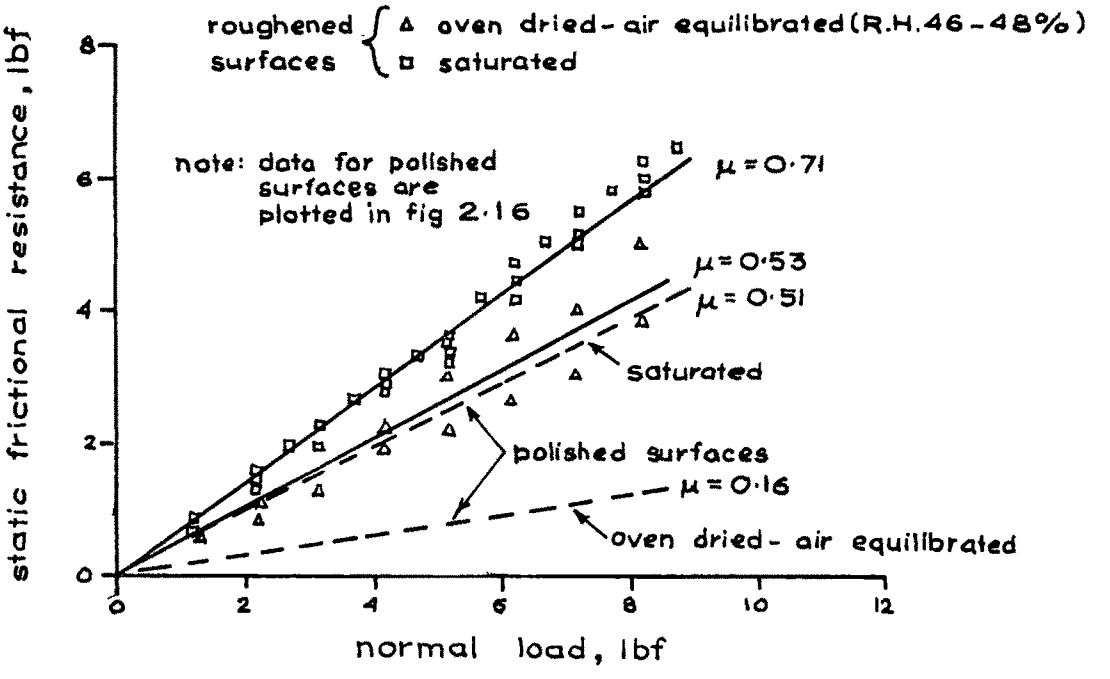

FIG. 2-17 THE EFFECT OF SURFACE ROUGHNESS ON THE FRICTIONAL CHARACTERISTICS OF MILKY QUARTZ (WISCONSIN)
(after HORN and DEERE, 1962).

2.5.2 Influence of normal stress

The value of coefficient of friction has been observed to vary with change in the value of the normal stress. The residual frictional force is not only due to pure sliding but is also influenced by the crushing of the broken asperities, rolling and induration into the crevices. The posibility of crushing increases with the increase in normal force and hence at higher normal stresses the movement is governed by turning of crushing pieces rather than due to shearing of the asperities. The following are the major findings of various workers.

(i) Handin and Stearns (1964) have found that the coefficient of friction at a higher normal stress is lower than at lower values of normal stress for dolomite, lime stone, and sand stone, consequent upon the surfaces becoming smoother at higher normal stresses.

(ii) Raleigh and Paterson (1965) found that the coefficient of friction of peridotite sliding on shear surfaces decreased with confining pressure.

(iii) Jaeger and Cook (1969 b) reported that for spherical trachyte contacts, sliding on trachyte with varying area of contact at higer normal loads, friction coefficient was 0.32 while at lower normal loads was 0.48.

(iv) Coulson (1970) showed that for all surface roughnesses, increase in normal pressure reduce the intial coefficient of friction from 5 to 20 %.

(v) Maurer (1966) while conducting test on sand stone lime stone, shale, marble, dolomite, granite and basalt at

various normal stresses found that the coefficient of friction when determined from residual shear resistance were dependent upon the normal stress and it decreases as contact pressure increases and showed relationship between friction coefficient and normal pressure by equation:

$$\tan \phi = a(\sigma_n)^k \qquad \ldots.2.5.1$$

The values of constants a and k are given in table 2.2.

TABLE 2.2

The values of a and k in equation 2.5.1

(after Maurer, 1966)

Rock type	a	k
Beekmantown dolomite	36.0	0.60
Berea sandstone	6.4	0.80
Carthage marble	29.0	0.63
Chico limestone	22.0	0.65
Georgia granite	46.0	0.55
Indiana limestone	60.0	0.46
Knippa basalt	48.5	0.56
Rush Springs sandstone	14.0	0.71
Seminole shale	3.7	0.73

(vi) Byerlee (1975) showed that the influence of normal stress could be considered by two straight lines or a parabola. At lower values, a power law best describes the shear and normal stress behaviour.

(vii) Drennon and Handy (1972) observed that at low normal stresses the value of static coefficient of friction

very considerably depending upon the past frictional history of the specimen.

(viii) Patton (1966 a) observed that at high normal loads a large reduction in strength occurs with small displacements while at lower normal loads displacement can be much greater before a drastic reduction in strength occurs figure 2.18.

In view of the above findings it can be deduced that the frictional value is a function of normal load.

2.5.3 Influence of water

A number of investigations have been carried out as regards the influence of water. The following are the major findings of the investigations.

(i) Tachebotarioff and Welch (1948) found that there is an appreciable difference between the friction values under dry and moist condition and the slightest humidity in the surroundings rapidly influences the friction results. This difference has been attributed to adsorbed water layer on the surface of the materials. (Table 2.3)

(ii) Horn and Deere (1962) found that the friction coefficient of oven dried surfaces to those of oven dried air equilibrated surfaces did not differ much for the massive structure minerals but a distinct difference existed for the layer lattice minerals. (Table 2.4) The differential behaviour has an explanation in the work of Hardy and Hardy (1919) according to which the action of water reduces the mobility of the adsorbed film composed of highly oriented molecules.

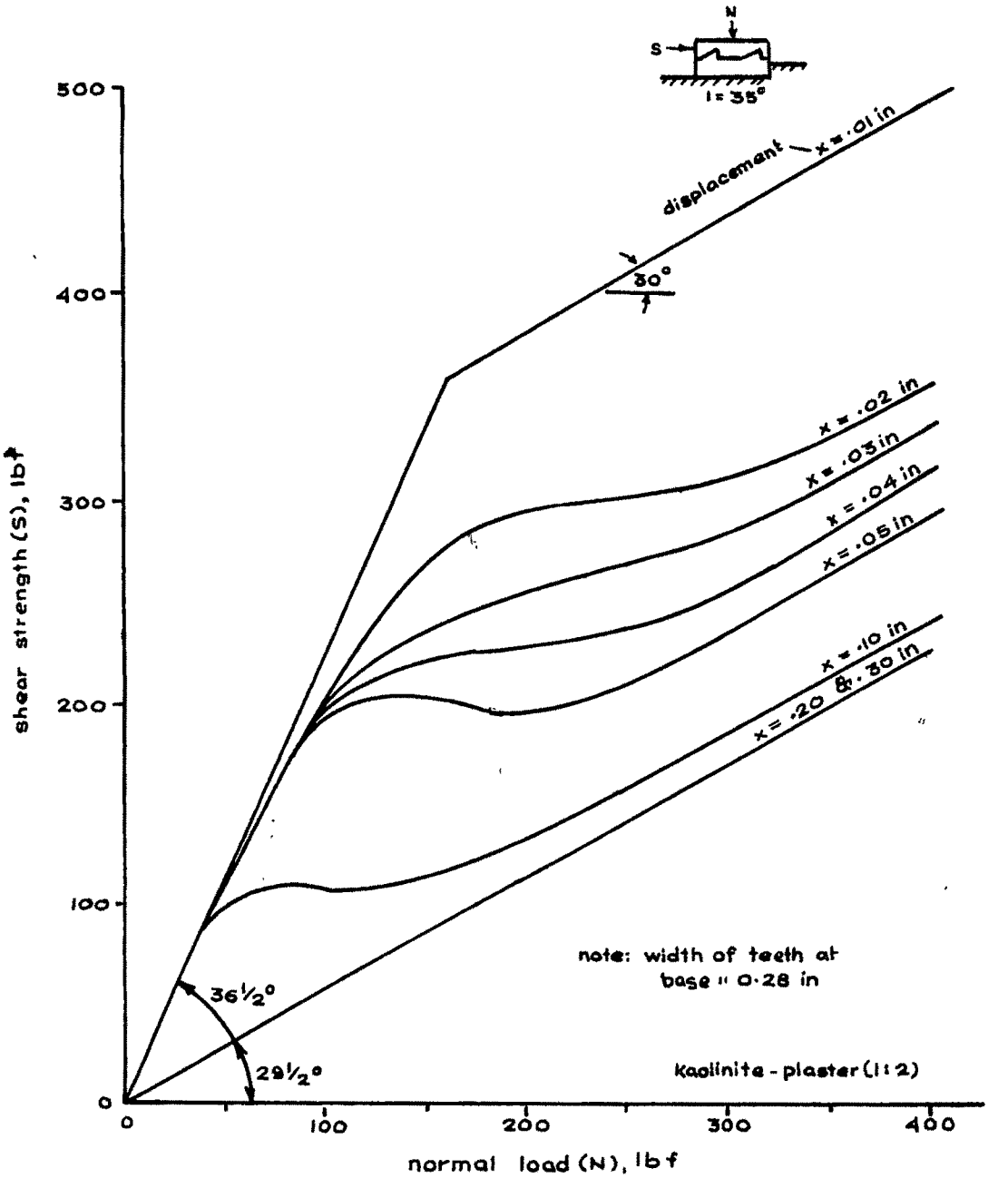

FIG. 2-18 SHEAR STRENGTH-DISPLACEMENT ENVELOPS
(after PATTON, 1966 a)

TABLE 2.3

Average values of friction coefficients obtained under dry and moist conditions (after Tschebotarioff and Welch, 1948)

Mineral	Dry[a]	Moist	Submerged
Quartz on quartz	0.106	0.455	0.455
Calcite on calcite	0.107	0.268	0.263
Pyrophyllite on pyrophyllite	0.163	0.120	0.122
Pagodite on pagodite	0.198	0.166	0.165
Quartz on calcite	0.098	0.266	0.333
Quartz on pyrophyllite	0.152	0.194	0.180
Quartz on pagodite	0.179	0.162	0.168
Calcite on pagodite	0.168	0.157	0.152
Calcite on pyrophyllite	0.233	0.127	0.134
Pyrophyllite on pagodite	0.179	0.113	0.113

[a]Dried in $CaCl_2$ desiccator and then quickly tested.

(iii) Menter (1950) showed by electron diffraction studies that the influence of disorientation of the molecules of a boundry lubricant may increase the frictional resistance.

(iv) Bromwell (1966) observed that the coefficient of friction of dry, chemically cleaned, polished quartz is 0.9 and remains uncharged when wetted, indicating that water is basically neutral to quartz and its antilubricating effect is due to its reaction with the lubricant layer.

TABLE 2.4

Frictional coefficients for three conditions of surface moisture

(after Horn and Deere, 1962)

	Mineral	Origin	Oven-dried		Oven-dried/ air-equilibrated		Saturated		$\frac{\mu_s^s}{\mu_d^s}$	$\frac{\mu_s^k}{\mu_d^k}$
			Static μ_d^s	Kinetic μ_d^k	Static μ_m^s	Kinetic μ_m^k	Static μ_s^s	Kinetic μ_s^k		
Massive-structured minerals	Clear quartz	N.Carolina	0.11	0.10	0.11	0.10	0.42	0.23*	3.82	2.30
	Milky quartz	Wisconsin	0.14	0.14	0.16	0.16	0.51	0.27*	3.64	1.91
	Rose quartz	Unknown	0.13	0.11	0.13	0.11	0.45	0.26*	3.45	2.36
	Microcline feldspar	Unknown-A	0.11	0.11	0.13	0.11	0.76	0.76	6.90	6.90
	Microcline feldspar	Unknown-B	0.12	0.12	0.12	0.12	0.77	0.77	6.42	6.42
	Calcite (Scratching)	N. Jersey	—	—	0.21	0.21	0.60	0.60	—	—
	Calcite (N.S.)	N. Jersey	—	—	0.12	0.12	—	—	—	—
	Calcite (N.S.)	Kansas	0.14	0.14	0.14	0.14	0.68	0.68	4.85	4.85
Layer-lattice minerals	Muscovite	Penna.	0.43	0.43	0.30	0.30	0.23	0.23	0.54	0.54
	Muscovite	Brazil	0.41	0.41	0.32	0.32	0.22	0.22	0.54	0.54
	Muscovite	Unknown	0.45	0.45	0.36	0.36	0.26	0.26	0.58	0.58
	Phlogopite	Madagascar	0.31	0.31	0.25	0.25	0.15	0.15	0.48	0.48
	Phlogopite	Canada	0.29	0.30	0.22	0.22	0.16	0.16	0.55	0.53
	Biotite	Canada	0.31	0.31	0.26	0.26	0.13	0.13	0.42	0.42
	Chlorite	Vermont	0.53	0.53	0.35	0.35	0.22	0.22	0.42	0.42
	Serpentine	Vermont	0.62	0.62	0.50	0.47	0.29	0.26	0.47	0.42
	Serpentine	Unknown	0.76	0.76	0.65	0.65	0.48	0.48	0.63	0.63
	Steatite	N.Carolina	0.38	0.38	0.26	0.26	0.23	0.19	0.61	0.50
	Talc	Vermont	0.36	0.36	0.24	0.24	0.16	0.16	0.45	0.45

Notes – 1. The above coefficients are for very smooth surfaces.
2. These coefficients are based on a rate of sliding of 0.7 in/min.
3. The coefficients refer to the friction developed between surfaces of the same mineral, e.g., quartz on quartz.
4. Relative humidity during oven-dried/air-equilibrated tests ranged between 17% and 35%.
5. The normal load ranged between 0.65 lbf and 10.2 lbf.
* Denotes approximate coefficient of kinetic friction; based on average of maximum and minimum values of frictional resistance during stick-slip movement.

(v) Lambe and Whitman (1969) confirms the antilubricant influence of water. While Byerlee (1966) contends that the influence of the fluid is to increase attractive force between the surfaces due to the surface tension effect.

(vi) Horn and Deere (1962) investigated the influence of non-polar and polar fluids and reported that the influence of high polar fluids (water, ethylene glycole, amylamine) on frictional coefficient was much more than a non polar films (Carbon tetrachloride, decahydronaphthalene).

(vii) Jaeger (1959) working on soaked specimens of sand stone and granitic gneiss observed that there occurs rather slight decrease in coefficient of sliding friction.

(viii) Parikh (1967) working on varieties of materials ranging from sintred bronz balls, glass ballotino, quartz sand, feldspar sand with various pore fluid like water, glycol and detergents, observed that there is an effect of pore fluid on the coefficient of sliding friction.

(ix) Morgenstern (1970) demonstrated that the pore pressure greately influences the sliding force due to decreased value of normal force.

(x) Byerlee (1975) showed that law of effective stress holds good for jointed surfaces.

(xi) Goodman, Heuze and Ohnishi (1972) showed that due to pore pressures, very high pressure may develop when joint slide past each other.

(xii) Jaeger and Rosengren (1969) observed that polished surfaces are not affected by the presence of water while rough surfaces showed the slight decrease in friction values.

Table 2.5 gives a comprehensive work of various workers.

TABLE 2.5

Effect of water on the coefficient of friction of rock joints

(after Barton, 1973 a)

Rock type	Description of discontinuity	Dry Φ^0	Dry μ	Wet Φ^0	Wet μ	Reference
Quartzite	artificial, planar, polished (σ_n: 30–400 kgf/cm^2)					JAEGER and ROSENGREN (1969)
Shales, siltstones and slates	minor faults; smooth, polished or slickensided, graphite coated		no change in general			ROSENGREN (1968)
Shales, siltstones and slates	extension fractures; coated with limonite, pyrite, quartz					ROSENGREN (1968)
			reduction			
Granite, gneiss, sandstone	shear fractures from failure of intact specimens (σ_n: 100–2,500 kgf/cm^2)		0.71 0.52		0.61 0.47	JAEGER (1959)
		Φ_r		Φ_r		
Sandstones, carbonates	artificial, rough sawn, equivalent to residual	25–34 33–39		24–33 32–36		PATTON (1966a)
Shales, siltstones and slates	minor fault, smooth, polished, chlorite coated		0.49		0.40	ROSENGREN (1968)
Dolerite	joint	52		37		DUNCAN (1969)
Granite	artificial surface	38		31		
Gneiss	natural schistose plane, "keyed"	49		44		
Phyllite	schistose plane	40		32		
Shale	joint	37		27		
Quartzite	joint	44		34–37		DUNCAN and SHEERMAN-CHASE (1965–66)
Marble	joint	49		42		
			increase			
Sandstone	artificial, planar, polished (equivalent to slickenside)	Φ_r 27–32		Φ_r 30–38		PATTON (1966a)
Gabbro	joint	47		48		
Oolitic limestone	joint	44		48		DUNCAN
Chalk (2 of 3 types)	joint	40		41		(1969)
Quartzite	artificial, planar, polished	23		30		DUNCAN and
Basalt	artificial, planar, polished	33		35		SHEERMAN-CHASE (1965–66)
Schistose gneiss, granite, sandstone	artificial, planar, polished with increasing polish during shear	—	—	—	—	COULSON (1970)

2.5.4 Influence of filling materials

It has been recognized that the mechanical behaviour of jointed rock filled with any material is dependent upon the type of the filling material, the thickness of the filling material and the height of the asperities. The following are the major findings as regards the influence of the filling material on behaviour of shear in jointed rocks.

(i) Goodman, Heuze and Ohnishi (1972) examined the influence of thickness of the filling material in granite and sand stone joints and showed that for very small thickness of the filling materials there is augmentation of the strength as a virtue of the geometry of the rough walls of the joints and as thickness is increased, the filling assume the strength to that of the filling material. (Fig. 2.19)

(ii) Barton (1973) related the mean thickness of the filling and the mean roughness amplitude and displacement required for rock to rock contact of joint walls. (Table 2.6)

TABLE 2.6

Relationship between joint filling, roughness amplitude at zero dilation to obtain displacement of joint wall contact. (after Barton, 1973 a)

f/a	d/a	
1.00		f = thickness of
0.75	2.34	filling
0.50	1.32	a = roughness
0.25	0.43	amplitude
0.00	0.00	d = displacement

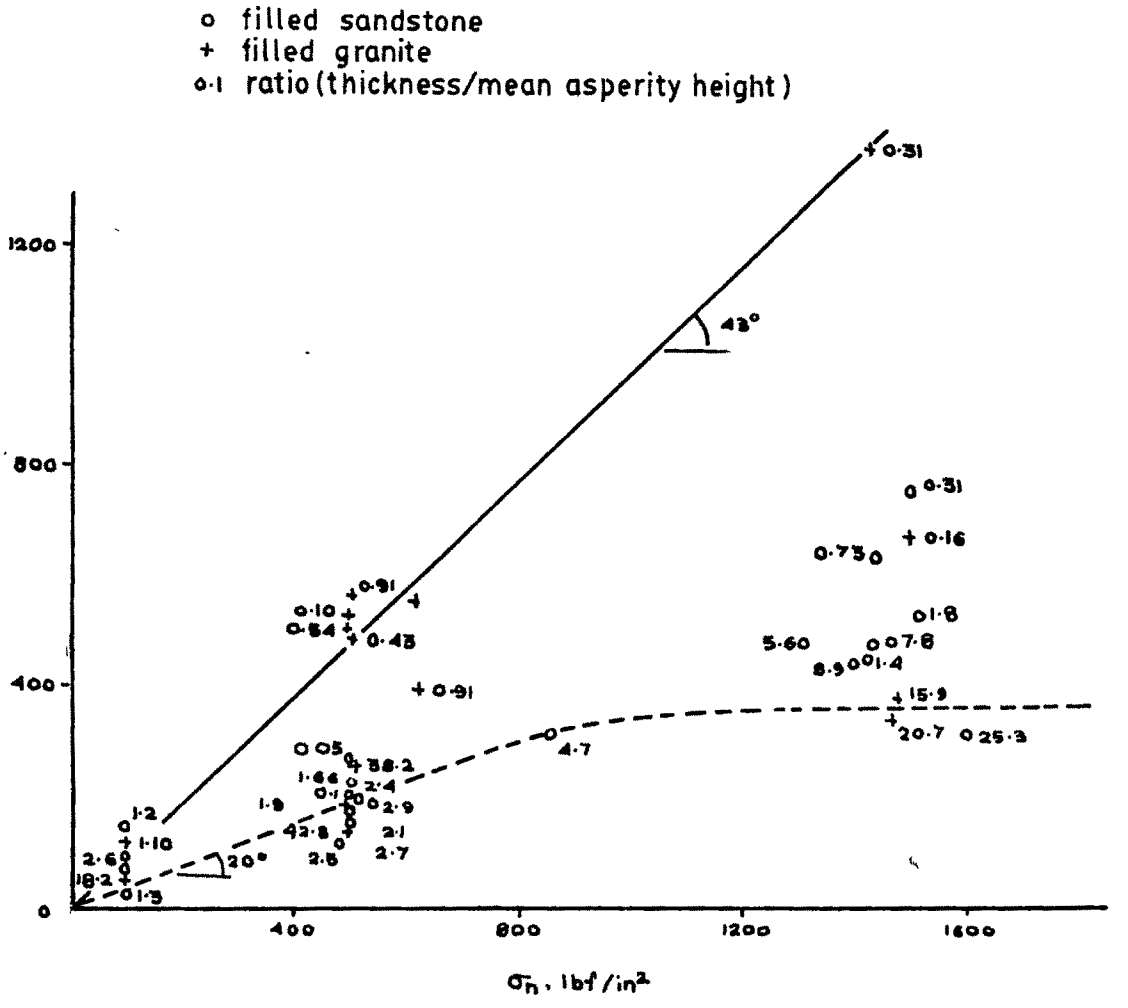

FIG. 2-19 STRENGTH DATA FOR CLAY FILLED JOINTS
(after GOODMAN, HEUZE and OHNISHI, 1972)

(iii) Tulinov and Molokov (1971) reported that a thin sand soil layer as a filler between the hard rocks, (sand stone, lime stone) does not have any significant influence but in case of relatively weak rocks, clay and marl, its influence is rather to increase the angle of friction. The influence of clay bonds is very much affected by the presence of humidity. With increase in humidity a drop in shear strength is observed. (Fig. 2.20 and 2.21)

(iv) Skempton and Hutchinson (1969) and Bjerrum (1973) revealed that the long term strength may be 10 to 15 % lower than that in over consolidated clays, the reduction in strength may be taken as 0.5 % to 2 % per log cycle of time. (Fig.2.22)

(v) Handin (1972 a,b) investigated the influence of the gouge compositian on the shear of the joint and found that the specimens with limestone sand are stronger than quartz sand and the relative ductility of the gouge is an important parameter. (Fig. 2.23)

(vi) Coulson (1970) examined artifical tension in coarse and fine grained granite with grout fillings of 0.80 to 6.4 mm (Fig.2.24) and showed that peak and ultimate strength reduces at higher normal stress but at lower values the peak strength of the joints is higher than the natural joints.

(vii) Borroso (1970) showed from the results on planar surfaces that there is an improvement in friction angle from 25° to 30° after grouting while in the case of shale there was no improvement. If the shear strength is higher than rock, the rock will control the shear strength and vice-versa.

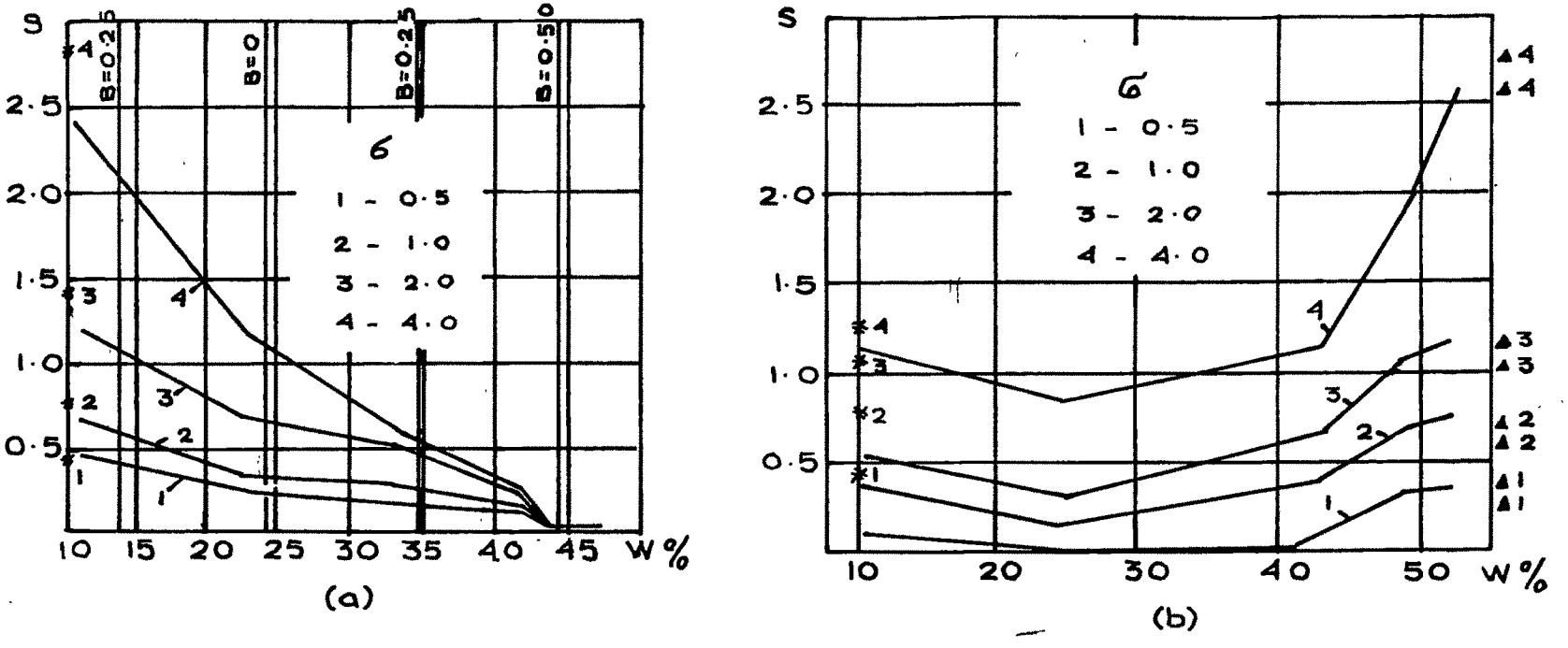

FIG. 2-20 (a) THE RELATION OF THE SHEAR STRENGTH TO THE HUMIDITY OF THE CLAY INTERBED (R=5mm) BETWEEN THE SANDSTONE PLATES. S= THE SHEAR RESISTANCE OF SANDSTONE PLATES ON SANDSTONE. B = CONSISTENCY INDEX, R = THICKNESS OF FILLING MATERIAL.

(b) RELATION OF THE SHEAR STRENGTH TO HUMIDITY OF GROUND CLAY SLATE (R = 6 mm) BETWEEN THE PLATES OF LIMESTONE & SANDSTONE AT POSSIBLE SOIL EXTRUSION. S = SHEAR STRENGTH OF UNDISTURBED · CLAY SLATE BETWEEN THE PLATES OF LIMESTONE AND SANDSTONE. SHEAR STRENGTH OF LIMESTONE PLATES ON SANDSTONE. Δ: ON DRY SURFACE (W=1·7%) ▲: ON MOISTENED SURFACE. W = PERCENTAGE OF WATER.

(after TULINOV and MOLOKOV, 1971)

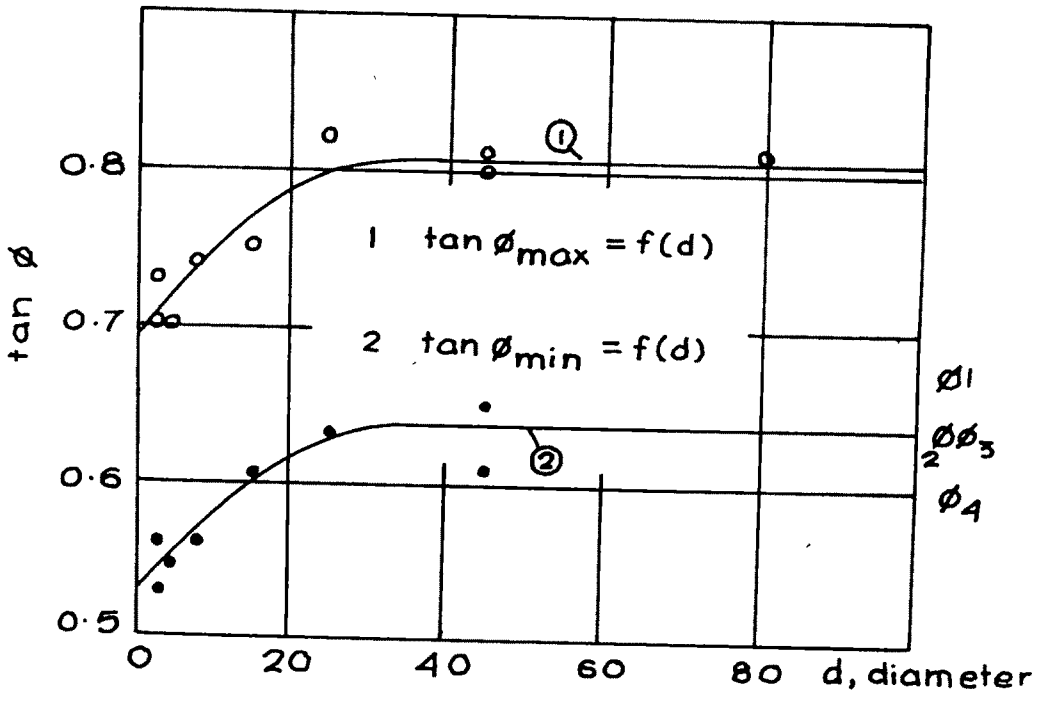

FIG.2·21 COEFFICIENT OF INTERNAL FRICTION FRAGMENTS DIAMETER RELATION Ø LUMP TEST RESULTS
1 - SANDSTONE ON SANDSTONE
2 - LIMESTONE ON SANDSTONE
3 - LIMESTONE ON SANDSTONE WITH FINE GRAINED SAND BETWEEN THEM
4 - LIMESTONE ON MOISTENED SURFACE
(after TULINOV and MOLOKOV, 1971)

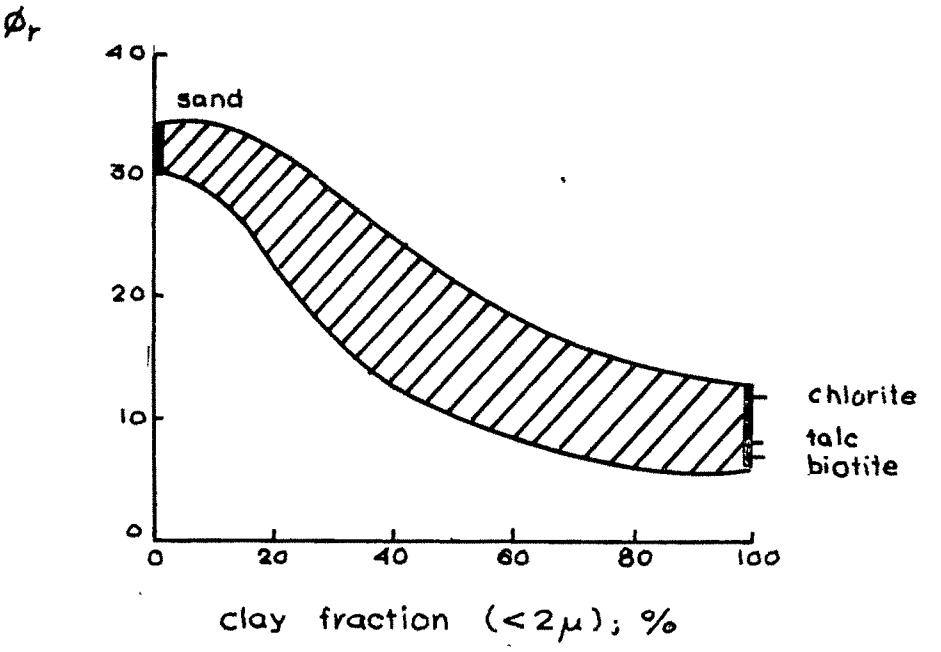

FIG. 2-22 DEPENDANCE OF RESIDUAL SHEAR STRENGTH ON CLAY FRACTION
(after SKEMPTON, 1964)

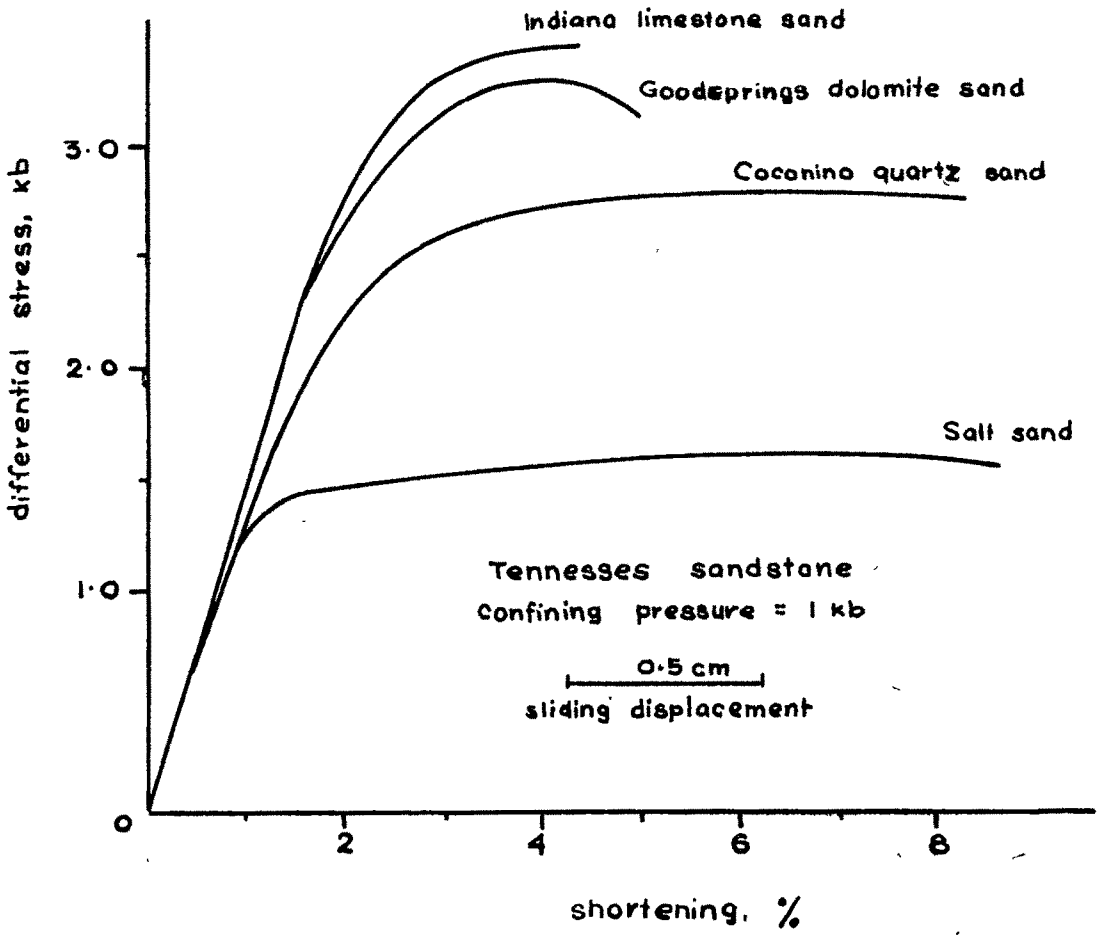

FIG. 2-23 DIFFERENTIAL STRESS VERSUS SHORTENING CURVES FOR TENNESSEE SANDSTONE WITH VARIOUS COMPOSITIONS OF GOUGE. EACH GOUGE ZONE WAS 0·15cm THICK. THE SPECIMENS WERE DEFORMED AT 1kb, ROOM TEMPERATURE AND A CONSTANT RATE OF SHORTENING OF 10^{-4} s.
(after HANDIN, 1972 b)

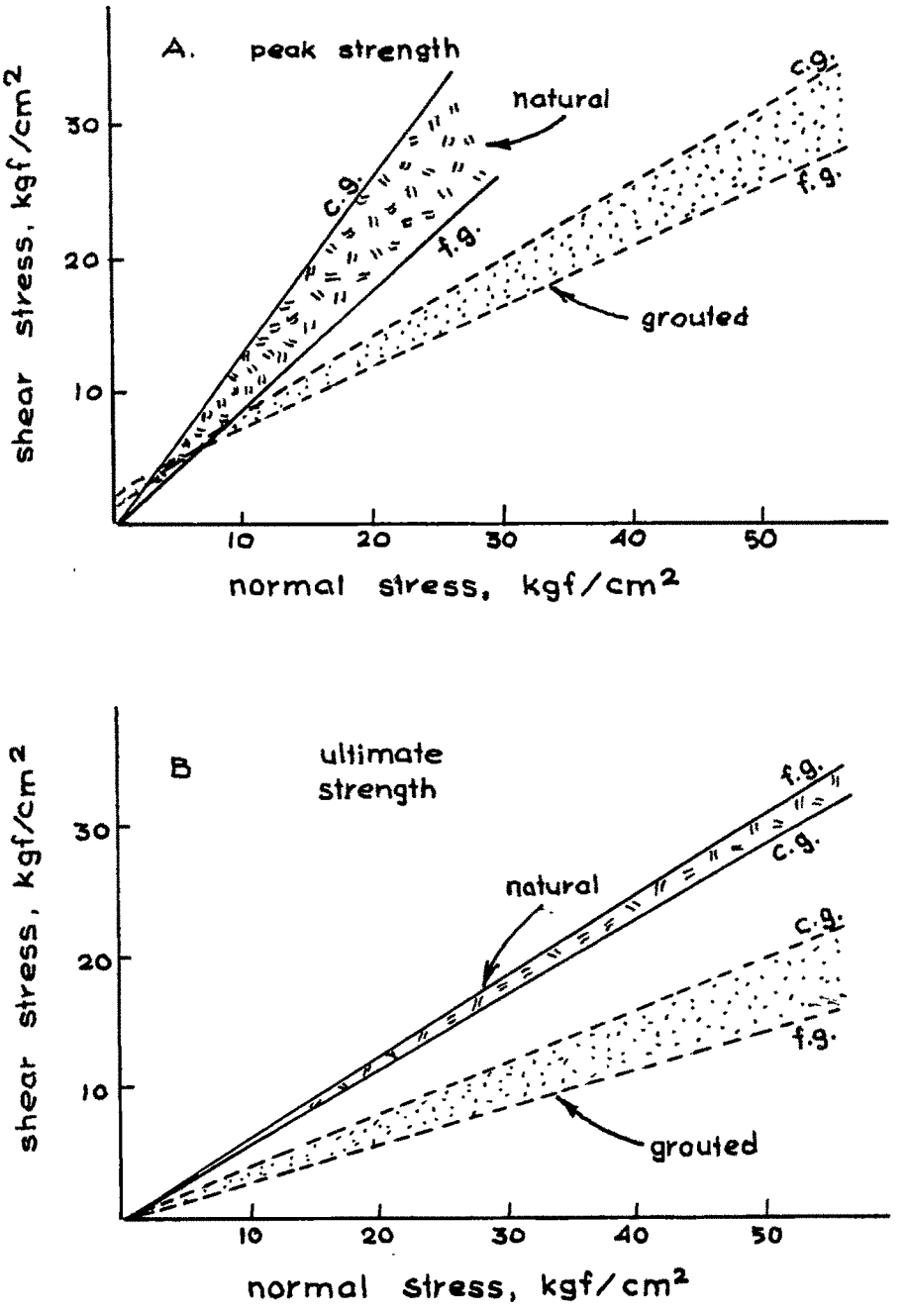

FIG 2 24 COMPARISSION OF PEAK & ULTIMATE STRENGTH FOR NATURAL AND GROUTED JOINT SURFACES FOR COARSE-GRAINED (c.g.) AND FINE-GRAINED (f.g.) GRANITE (after COULSON, 1970)

2.6.0. MECHANISM OF SLIDING BETWEEN JOINT SURFACES

2.6.1 Physical process of sliding of joint surface

The process of friction and sliding of rock surfaces have been investigated for joints with rock flour, gouge and gouge zones, polished areas and indurated crusts. Following are the major expositions from the various investigations.

(i) Byerlee (1966) examined the physical process of sliding between two blocks from the point of view of mechanism associated with brittle materials. He concluded that the interlocking of irregularities get sheared off as a result of developement of high tensile stresses. If the contact area is small the force required to shear the asperities is small and vice versa. The physical process involved in the sliding when the contact between the surfaces is confined to isolated regions is no different from the physical process when the contact is made over the whole of the surface.

(ii) Patton (1966) while examining the influence of the number of teeth observed that when two surfaces have asperities sheared off, the shearing force acts primarily on the external teeth and these are sheared off before the full length of the central teeth is sheared. The phenomenon of frictional sliding is thus of progressive failure of asperities with displacement and not the failure of all the asperities at one time.

(iii) Hoskins, Jaeger, Rosengern (1968) found a surface damage and slickenside of rough surfaces, while they observed stick-slip oscillations for smooth surfaces with practically no surface damage.

(iv) Jaeger (1971) while working on sliding of rough surfaces found that the contact is lost only where intense shearing and removal of material took place. At places of contacts where profuse gouge material is formed, the rubbing blocks may fail by indirect tension caused by local stress at contacts.

(v) Coulson (1970) examined the phenomena of surface damage and classified them to the catagories of polishing, induration and rock flour and gouge and further observed that gouging and generation of rock flour is chiefy associated with rougher and sand blasted surfaces (Fig. 2.25). Under microscope it is observed that the gouge material and rock flour consisted of small discrete angular particles indicating the absence of any plastic deformation. The compacted gouge flour in the gouge trough had the appearance of typical slikensides (Fig. 2.26) and chatter marks similar to those associated with rock abrasion. At the bottom of the gouge material step like features similar to the "RIEDEL shears" as per Cloos (1928) and Riedel (1929).

(vi) Einstein et al (1969) from the studies on jointed specimens found that the steep sides formed are opposed to the direction of sliding (Fig. 2.27) and whose steps are part of secondary conjugate shear planes along which displacement occurs after the primary shear surface has been created. However this phenomenon has been found to be absent at higher confining pressures.

(vii) Handin (1972 b) found that the gouge developement changes systematically. The abundance of thick, clumped gouge

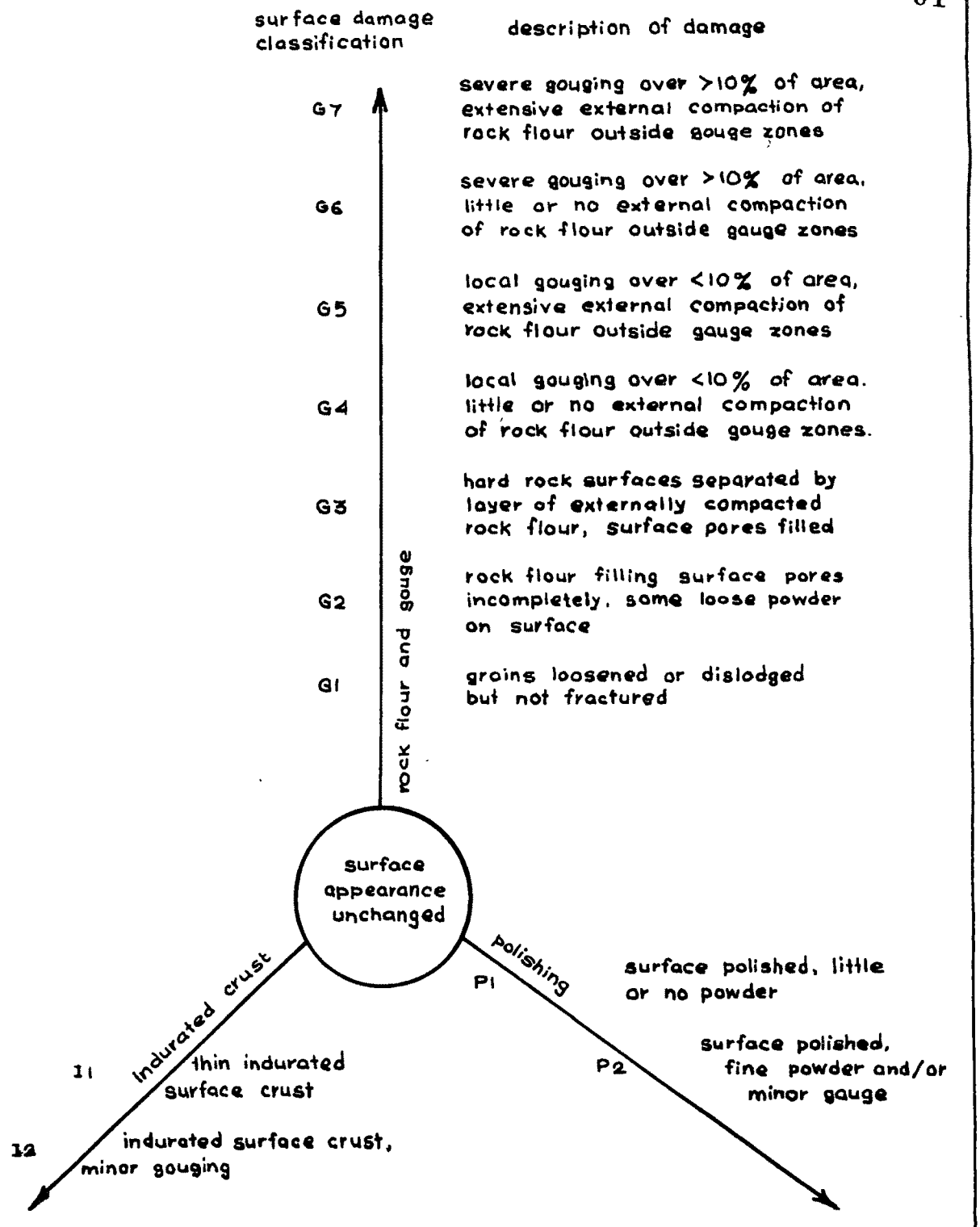

FIG.2-25 SURFACE DAMAGE CLASSIFICATION SYSTEM
(after COULSON, 1970)

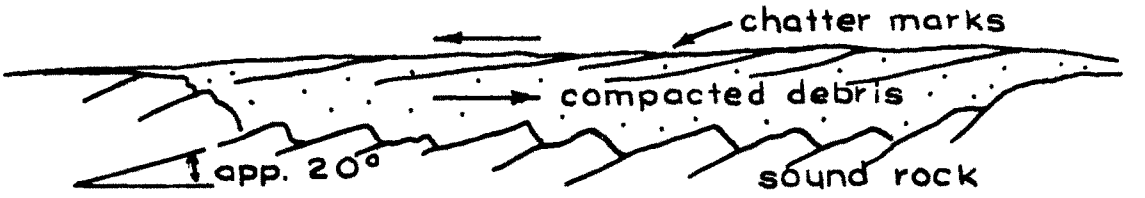

FIG.2·26 SCEMATIC CROSS SECTION OF GOUGE ZONE DEVELOPED ON A SOLENHOFEN LIMESTONE SURFACE SHEARED DRY UNDER NORMAL PRESSURE OF 1177 lbf/in^2
(after COULSON, 1970)

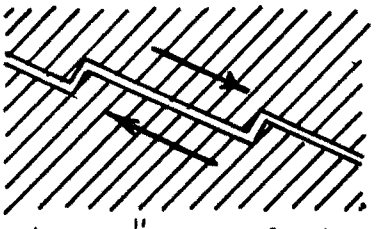

observed "steps" on failure surface and direction of movement

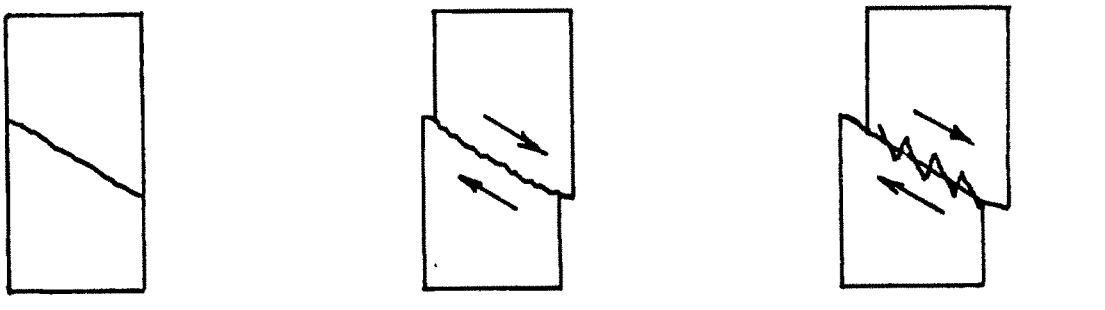

failure

beginning of residual sliding

residual sliding and formation of secondary shear planes

FIG.2·27 FAILURE SURFACE DEVELOPMENT
(after EINSTEIN et al 1969)

increases while undisturbed original surface and "welded gouge" decreases with increase in precut angle to the direction of axial load may be due to change in normal pressure on the sliding plane. He found gouge abundance with increase in confining pressure however there is no perceptible influence of strain rate (Fig. 2.28).

(viii) Coulson (1970) concluded that the phenomenon of induration of the surface is associated with an extensive amount of "cut and fill" in the original rock surface.

2.6.2 Phenomenon of dilatation

Dilatation has been considered as a significant phenomenon in case of shearing behaviour of jointed rocks. The most commanly used method for representing the dilatation is the vertical displacement against the horizontal displacement. The amount of vertical displacement at any instant is dependent upon the relative position of the different asperities of the sliding surface (Fig. 2.29). Another method of representation is the relationship between the vertical displacement with respect to the horizontal displacement expressed in terms of dimensionless stress ratio such as (τ/σ_n) or (σ_n/σ_c). Barton (1971 a) conducted a series of model tests on tension joints using a model material and found that there exist a linear relation of peak dilation angle α_n and the peak stress ratio $\tan^{-1}(\tau/\sigma_n)$ (Fig.2.30) which can be represented by a relationship

$$\tau/\sigma_n = \tan(1.78\alpha_n + 32.88^\circ) \qquad \ldots.2.6.1$$

Barton also tested model joints at various normal stresses depending upon the relative compressive strength

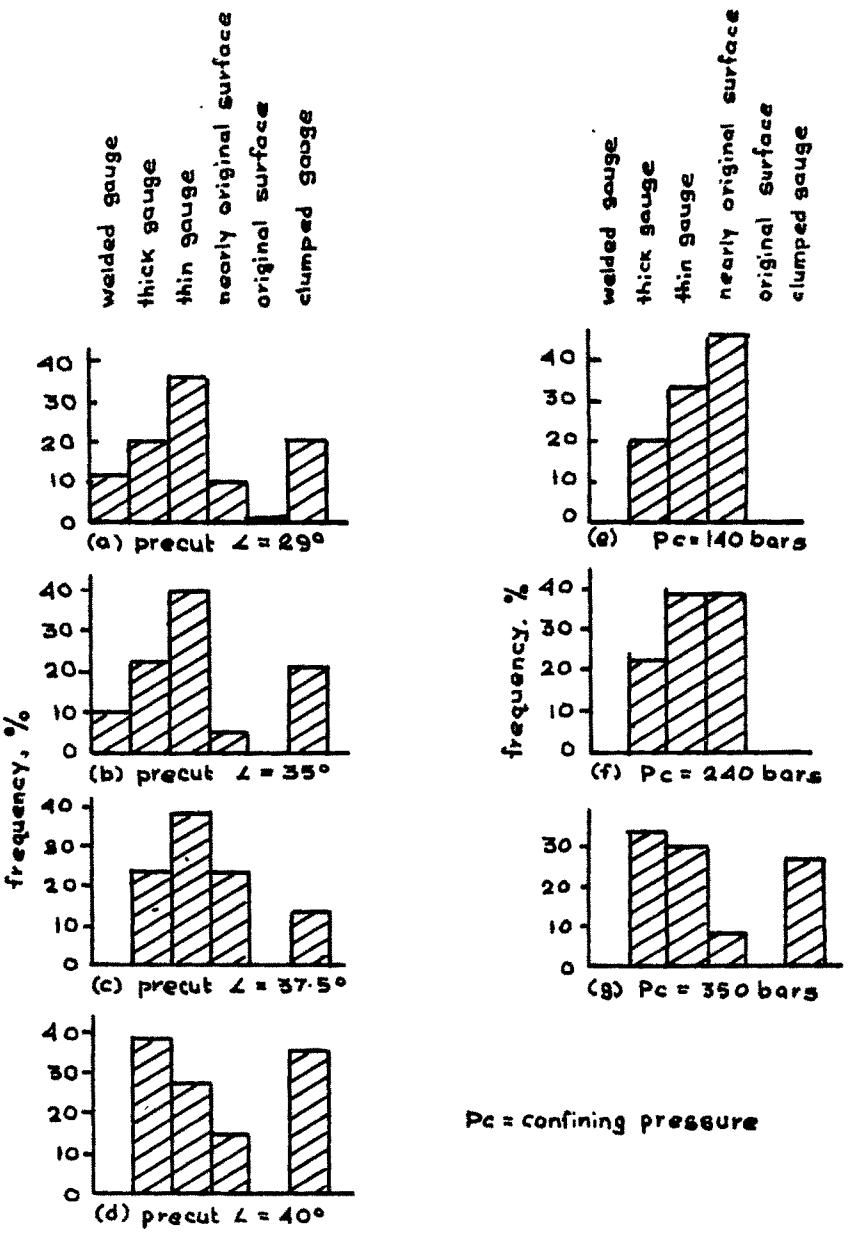

FIG.2-28 HISTOGRAMS SHOWING GOUGE DEVELOPMENT IN FRICTIONAL GLIDING EXPERIMENTS TENNESSEE SANDSTONE. FRIQUENCY IN THE OCCURRENCE OF GOUGE TYPES ARE BASED ON POINT COUNTING METHOD; TOTAL COUNTS ARE 423, 358, 290 240, 330, 300 & 282 IN HISTOGRAMS a-g, RESPECTIVELY. (a-d) HISTOGRAMS SHOW GOUGE CHANGES FOR INCREASE IN ANGLE OF PRECUT, IN TESTS RUN AT 140 BARS CONFINING PRESSURE, 24°C, 10^{-4}/s. INITIAL SURFACES WERE PREPARED WITH GRINDER ONLY. (e-g) HISTOGRAMS SHOW GOUGE CHANGES FOR INCREASING CONFINING PRESSURE AT FIXED PRECUT OF 35°. INITIAL SURFACE PREPARED WITH GRINDER PLUS POLISHING WITH 600 GRIT ABRASIVE.

(after HANDIN, 1972 b)

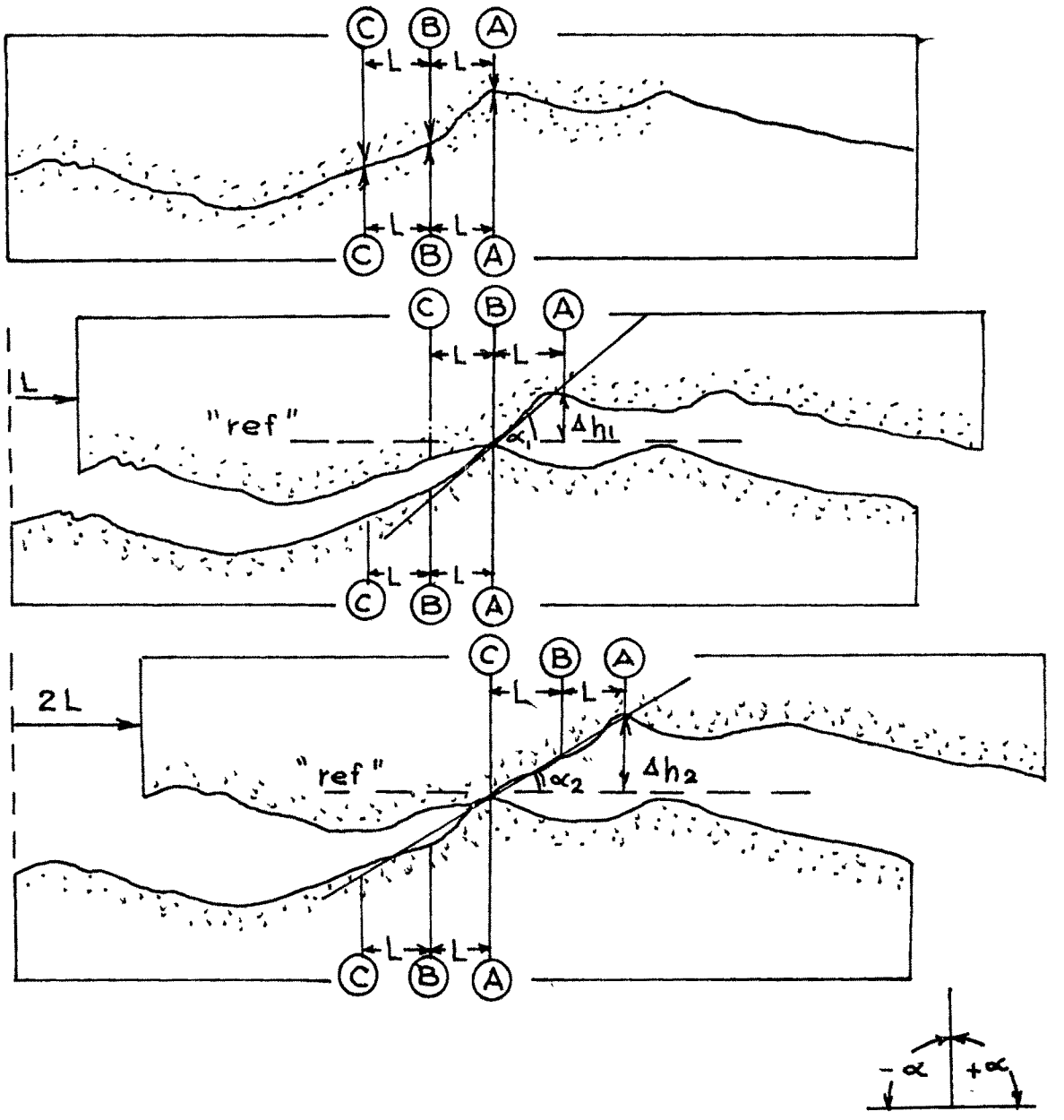

FIG. 2·29 RELATIONSHIP BETWEEN SURFACE GEOMETRY AND DILATATION DURING SHEAR DISPLACEMENT
(after FECKER and RENGERS, 1971)

of the material and found that the dilation angle decreases with increase in the ratio of σ_n/σ_c. The relationship is linear on a logarithmic scale (Fig. 2.31) and expressed as

$$\log_{10}(\sigma_n/\sigma_c) = -0.1056\,\alpha_n + 0.1184 \quad \ldots.2.6.2$$

or

$$\log_{10}\sigma_n/\sigma_c = -0.1\alpha_n \quad \ldots.2.6.3$$

or

$$\alpha_n = 10\log_{10}(\sigma_c/\sigma_n) \quad \ldots.2.6.4$$

The results of above equation 2.6.4 are given in table 2.7

TABLE 2.7

Results of equation 2.8

(after Barton, 1971 b)

σ_c/σ_n	α_n, degrees
1.0	0
10	10
100	20
1000	30

2.6.3 Phenomenon of stick-slip

The phenomenon of stick-slip has been characterized as a relaxtion oscillations occuring when the coefficient of kinetic friction is less than the coefficient of static friction. Several investigations have been conducted on this phenomenon especially in case of metal friction, but in case of brittle material like rock there are but few studies.

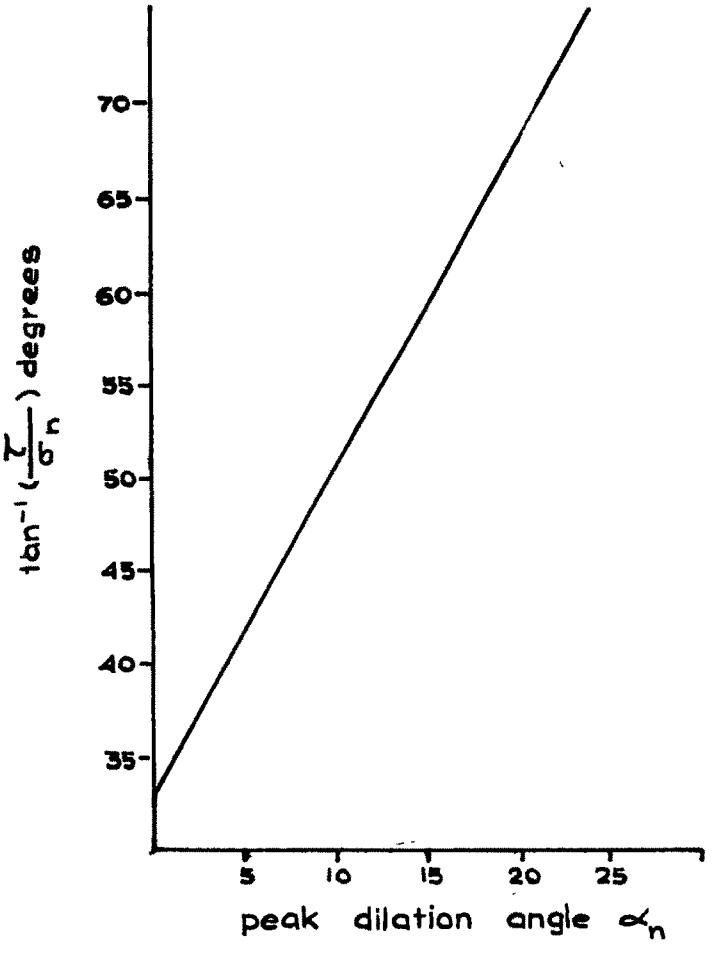

FIG. 2·30 LINEAR VARIATION OF PEAK DILATION ANGLE WITH PEAK STRESS RATIO.
(after BARTON, 1971 b)

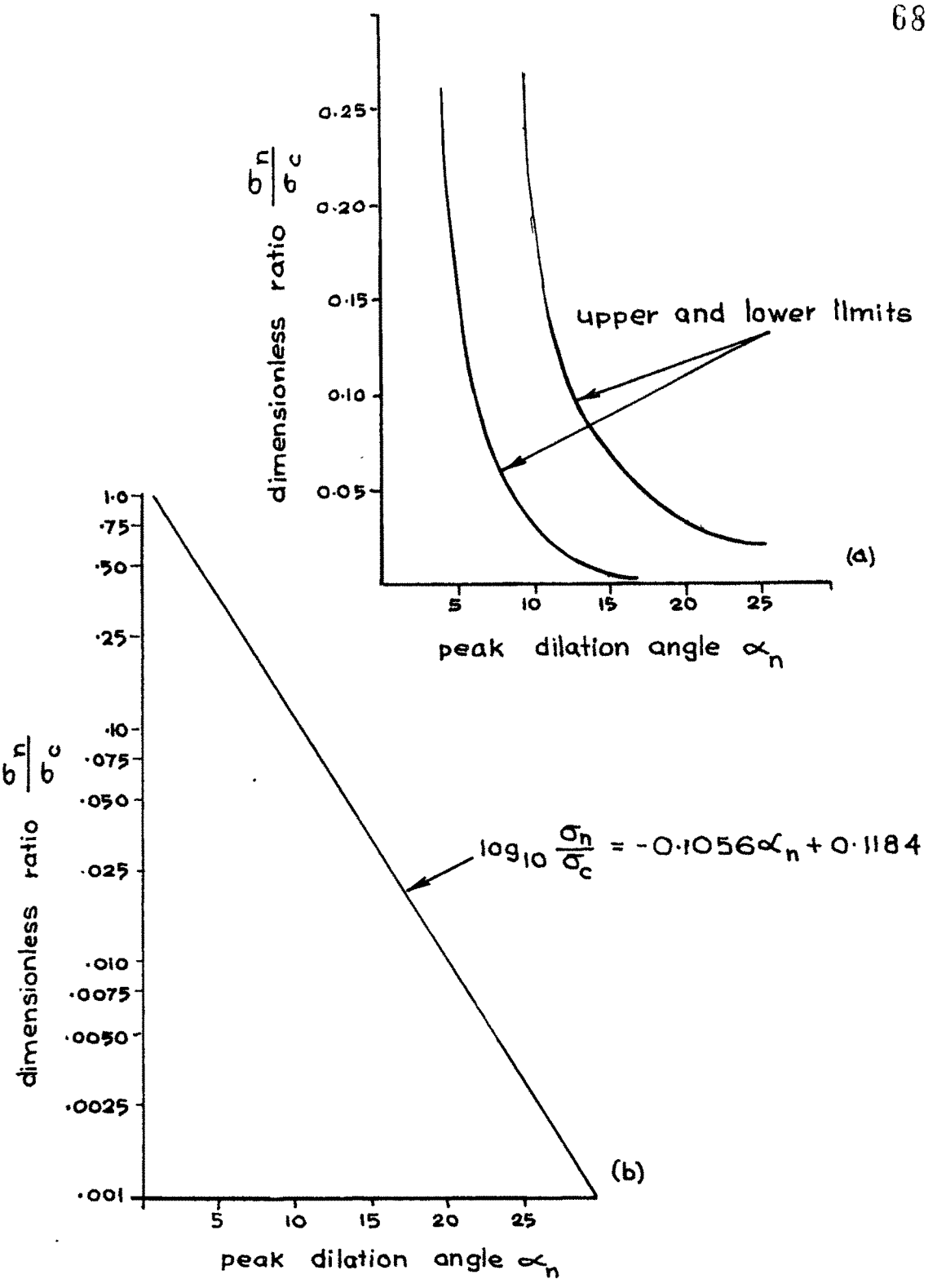

FIG. 2-31 (a) VARIATION OF PEAK DILATION ANGLE WITH RATIO OF NORMAL STRESS TO COMPRESSIVE STRENGTH.

(b) LINEAR VARIATION OF PEAK DILATION ANGLE WITH LOGERITHMIC RATIO OF NORMAL STRESS TO COMPRESSIVE STRENGTH
(after BARTON, 1971 b)

(i) Bridgman (1936) was the first to report this phenomenon while shearing brittle materials at normal stresses and observing jerky movement within the surface and a sudden drop in the value of shearing force.

(ii) Jaeger (1959) from tests on flat surfaces observed that after short initial period of sliding, subsequent movement takes place by violent stick-slip process of large amplitude (Fig. 2.32).

(iii) Byerlee (1966) working on westerly granite found that at the end of displacement the shear force in most cases dropped to about 2/3 of the shear stress required to initiate the movement. Christensen et al (1974) confirmed the observations using torsional shear test on ground Westerly granite.

(iv) Hoskins, Jaeger and Rosengern (1968) reported that in case of red granite with lapped surfaces after initial rise in load a sudden slip occurs and stick-slip proceeded regularly with increasing amplitude (Fig. 2.33). They further observed that these were associated only with surface of high finish and behaviour can be inhibited by reworking of the surfaces.(Fig. 2.33 and Table 2.8).

(v) Brace and Byerlee (1966 a,b) and Byerlee (1967 a) stated that these oscillations are more pronounced with rough surfaces than smooth surfaces.

(vi) Handin (1972 a,b) indicated that for stick-slip to occur the rock should not be of carbonite composition nor should contain alteration products of high ductility. Further he observed that the sliding surface should be flat, planar, free from large interlocking asperities and should be devoid of gouge material(Fig.2.34)

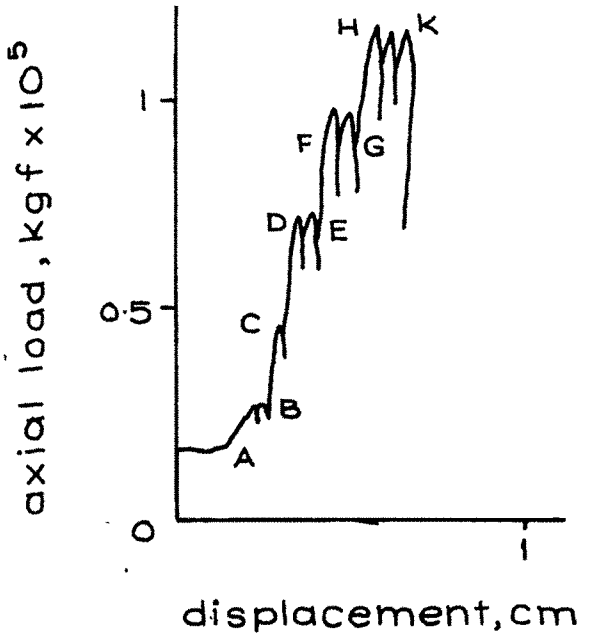

FIG. 2·32 LOAD DISPLACEMENT CURVE FOR SLIDING OVER BARE SURFACES AT $\alpha = 25°$. (α = ANGLE OF INCLINATION OF PRECUT WITH THE AXIAL FORCE)

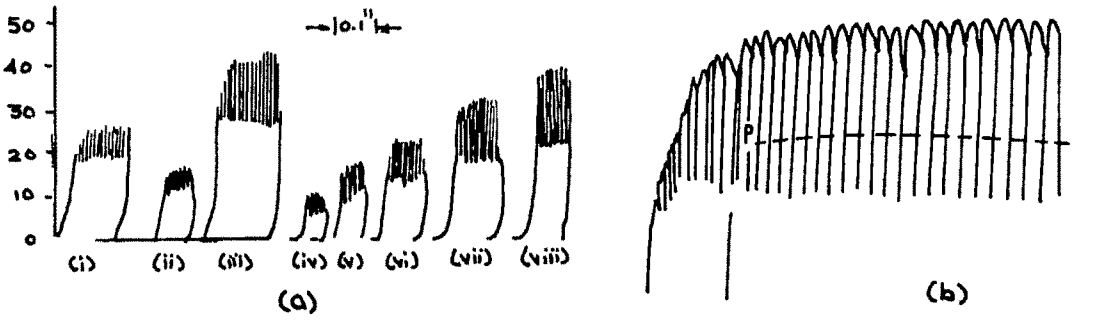

FIG. 2·33 (a) TESTING MACHINE RECORDER LOAD DISPLACEMENT CURVES FOR SMOOTH. RED GRANITE WITH SURFACE ROUGHNESS 35±5 μin. FLAT JACK PRESSURES.
(i) 500 lbf/in^2; (ii) 250, (iii) 750, (iv) 125, (v) 250, (vi) 375 (vii) 500 & (viii) 625.

(b) THE OSCILLATIONS OF FIG. 2·33 (a)(i) ON A MAGNIFIED SCALE.

(after HOSKINS, JAEGER and ROSENGREN, 1968)

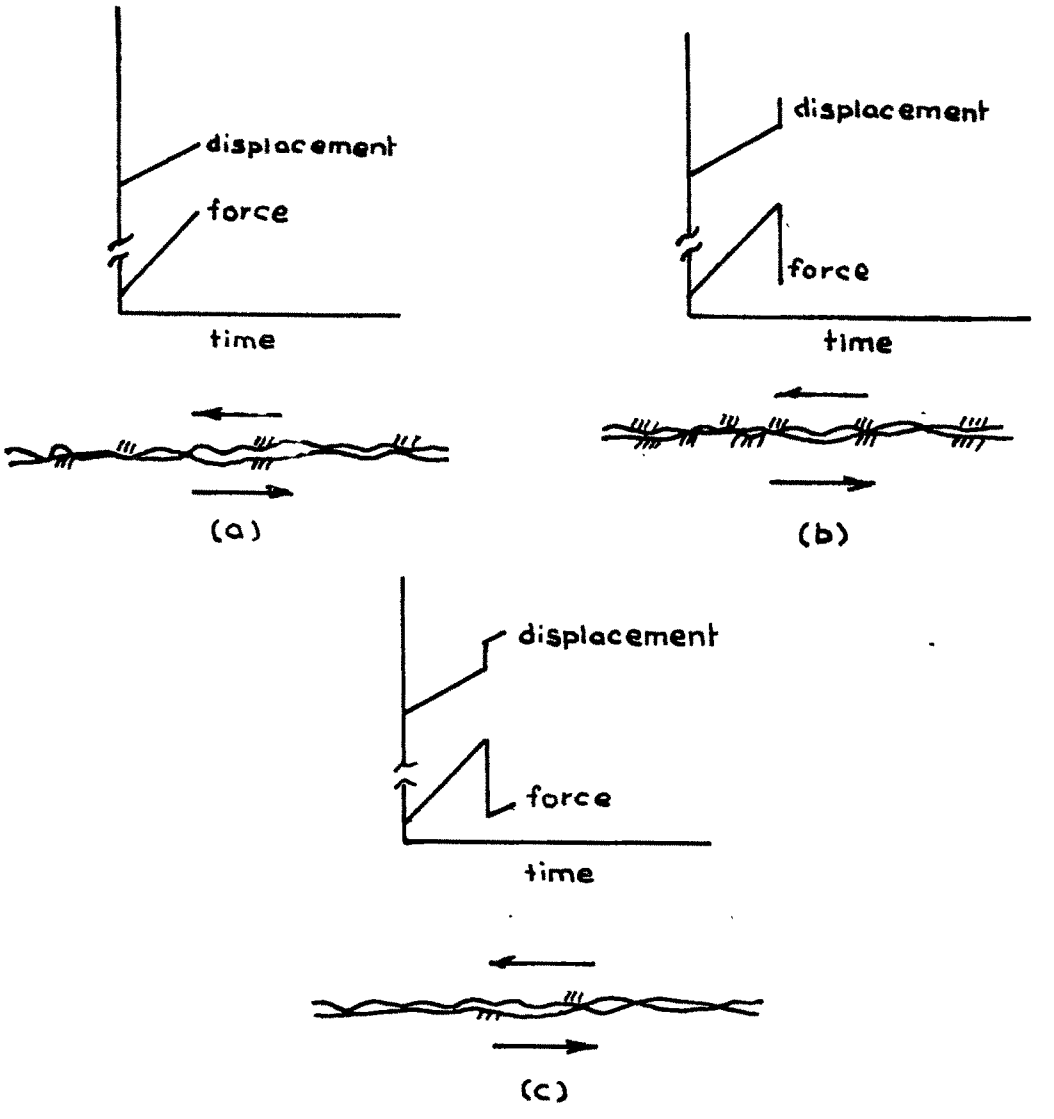

FIG. 2-34 SCHEMATIC DIAGRAMS OF CONCEPT OF SURFACE DEFORMATION DURING STICK SLIP. SHADED AREAS INDICATE ELASTIC STRAINING OF ROCK AT SLIDING SURFACE.
(after HANDIN, 1972 b)

TABLE 2.8

Coefficient of friction and cohesion for rock surfaces exhibiting stick-slip behaviour (after Hoskins, Jaeger and Rosengren, 1968)

Rock	Surface roughness uin(u cm)	u	u^*	u'	c	c^*	$(F-F^*)/X$ lbf/in (N/m)
Red granite	35±5 (89±13)	0.53	0.31	0.42	40	40	5.1×10^6 (894×10^6)
Red granite	80±20 (203±51)	0.53	0.48	0.50	50	50	4.7×10^6 (823×10^6)
Gabbro	35±5 (89±13)	0.32	0.25	0.28	35	30	3.4×10^6 (596×10^6)
Gabbro	50 (127)	0.18	0.15	0.16	40	30	2.9×10^6 (508×10^6)
Trachyte	30 (76)	0.63	0.54	0.58	60	70	5.0×10^6 (876×10^6)
Carrara marble	55 (140)	0.41	0.39	0.40	120	110	

u = coefficient of friction before slip

u^* = coefficient of friction after slip

u' = average value of coefficient of friction equal to coefficient of dynamic friction

c = intercept on axis before-slip curve

c^* = intercept on axis after-slip curve

$\frac{F-F^*}{X}$ = stiffness of the machine

F = load before slip

F^* = load after slip

X = displacement during slip

(vii) Logan et al (1973) observed in triaxial test that slip is enhanced when the sliding surface makes an angle 30° to 40° to the load axis.

(viii) Byerlee and Brace (1968) investigating the influence of various factors such as rock type, pressure, strain rate and stiffness of the system on phenomenon of stick-slip found that certain rock types (granite, gabbro, granodiorite, dunite) give rise to stick-slip and stick-slip amplitude increases with increase in confining pressure. Fig.2.35. At low pressure rock slips, with stable sliding and only at intermidate and high pressure stick-slip happens. They concluded that stick-slip is controlled by mineral type and porosity. Stick-slip does not occur with high porosity rocks like tuff rock and with rock containing calcite, serpentine etc. They also confirmed the observation of Rabinowicz (1965) that the stiffness of the system has influence in the phenomenon of stick-slip and that very elastic system give rise to greater drop in stick-slip.

(x) Lama (1975 a) working on models of marble surfaces in a Brazilian test using plaster water mixture as model material showed distinct stick-slip phenomenon on highly rough surfaces as well as polished surfaces. He showed that the amplitude of stick-slip is related to the normal stress and the shear displacement rate (Fig.2.36)

(xi) Byerlee (1968 a) found that the gouge materials which is more or less granular undergoes compaction at high pressure and then dilates under shear indicating the mechanical instability which may be responsible for stick-slip.

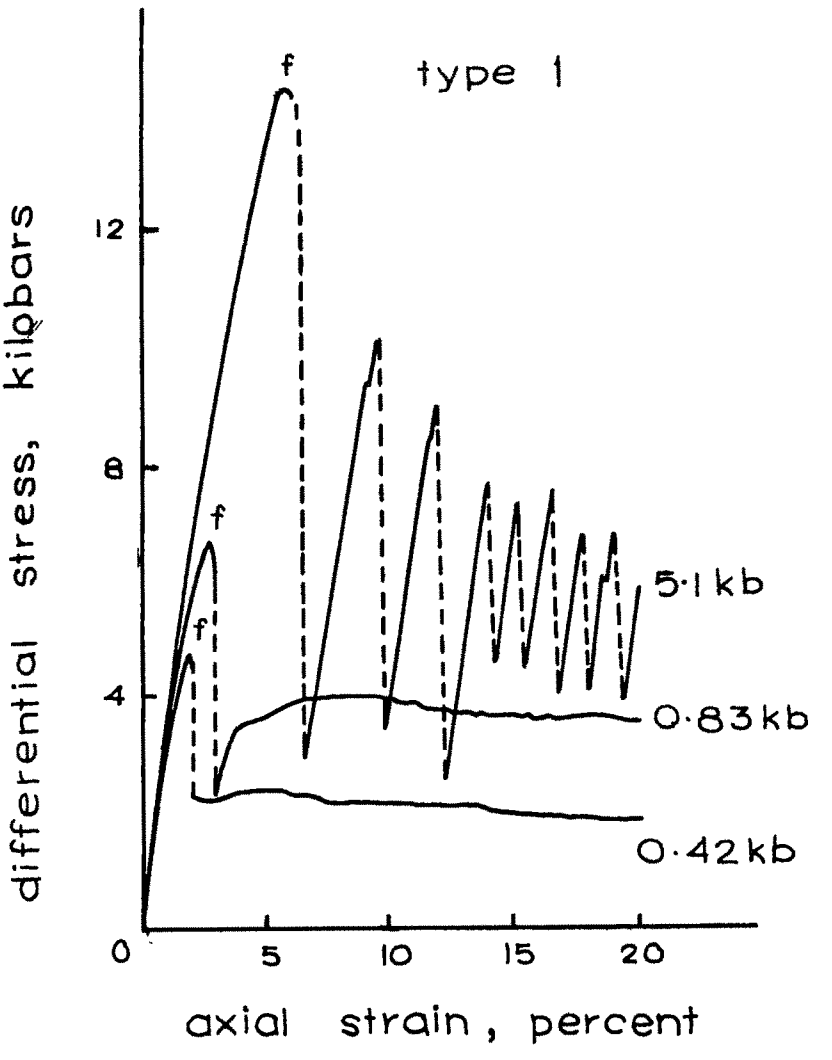

FIG. 2·35 DIFFERENTIAL STRESS VERSUS AXIAL STRAIN FOR SAN MARCOS GABBRO. THE VALUE AT THE END OF EACH CURVE GIVES THE CONFINING PRESSURE IN KILOBARS.

(after BYERLEE and BRACE, 1968).

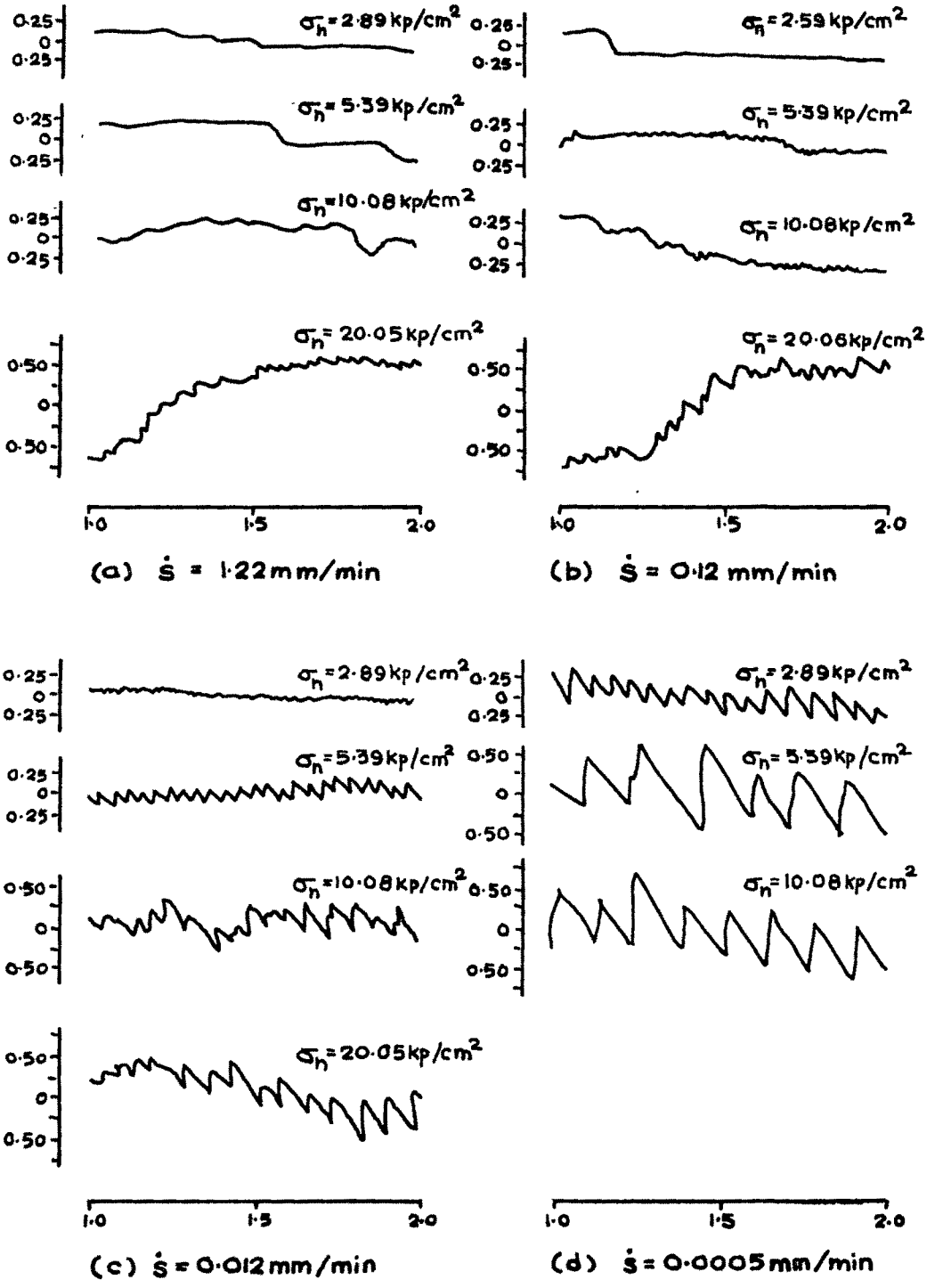

FIG. 2·36 STICK-SLIP AS A FUNCTION OF DISPLACEMENT RATE AND NORMAL STRESS IN THE DISPLACEMENT RANGES 1 to 2 mm.
(after LAMA 1975 a)

(xii) Scholz and Engelder (1976) working on diamond asperities on different rock surfaces supports the contention that the kinetic and static friction values should be velocity dependent.

It can be concluded that the mechanism of stick-slip may be divided into two distinct classes firstly the individual movements that are associated with the shearing of the asperities which owing to the stiffness of the loading system results in sudden drop in the shear force. Secondly, relaxation oscillations occur due to the difference in kinetic and static friction coefficient of the surface.

2.7.0. CONSTITUTIVE MODELLING OF ROCK JOINTS

2.7.1 Physical models

To expose the range of behaviour of jointed rock physical models capable to be representative into mathematical terms have been attempted. The most known model is that proposed by Dieterich (1981) to describe the constitutive properties of jointed rock simulating the experimental or field conditions.

The model is capable to reproduce the full range of effects in the laboratory experiments. In addition it produces the effect of the factors like mode of slip, stick-slip, slip or oscillatery slip. In qualitative sense most of the experimental data appeared to agree with the results obtained through testing. The model is based on a zero mass slider and spring system,(Fig. 2.37). The spring with stiffness K represents the combined elastic properties of the system. In this model the slider is externally loaded by

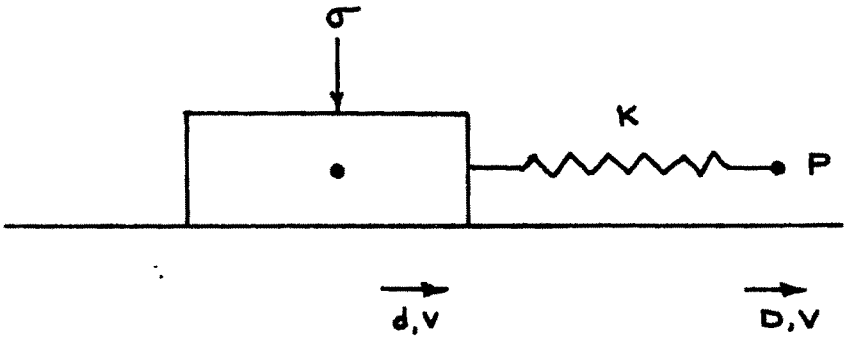

FIG. 2-37 SPRING AND SLIDER MODEL

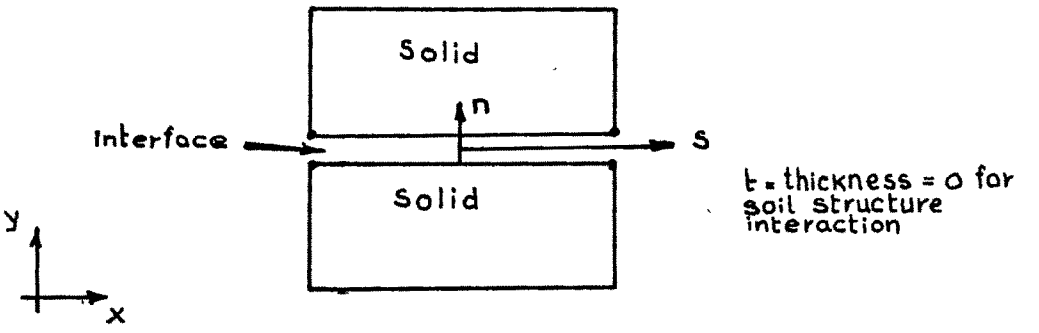

FIG. 2-38 a RELATIVE DISPLACEMENT ELEMENT[1]

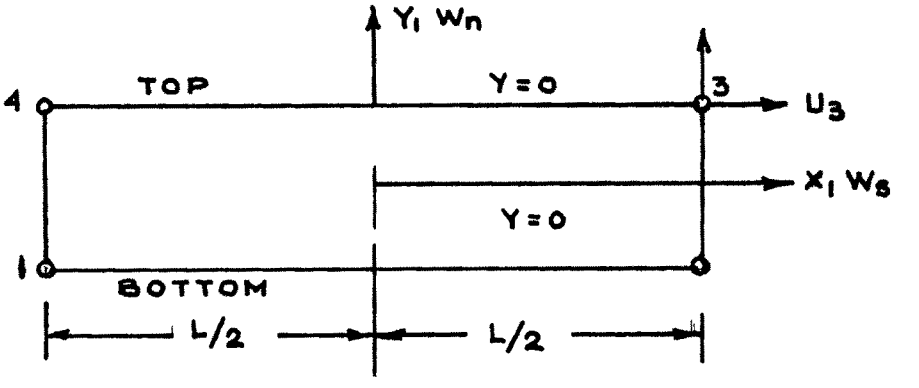

FIG. 2-38 b. JOINT ELEMENT, WIDTH = 0; LOCAL COORDINATE SYSTEM

specifying the displacement, velocity or loads. To simulate the conventional experimental situation, the motion of loading point correspond to the observed displacement. The computational procedure for this model is deterministic and uses a displacement marching scheme in which the slider velocity is assumed to be constant during each step. For each displacement step the principal unknown for computation is slider velocity. An iterative procedure is emplyed to find velocity and to find the friction force at the end of the step which equals the spring force. When the velocity is determined, the displacement then incremented and the iteration of the next step begins. Numerical computation using the Dieterich model of simple spring and slider are in good arrengement with the various experimental observations.

2.7.2 Joint elements

The developement of finite element method has provided a powerful tool for the analysis of structures in rock. Most importantly the finite element concept allows advanced mathematical models of rock specimen to be the building block in a representation of jointed rock mass. For analysing the behaviour of jointed rock it is proposed to treat jointed rock as an aggreate of massive rock blocks separated by joints with constitutive properties.(The chronological development of joint elements is described as per table 2.9.)

The most joint models are planar. Also the most joints are assumed to have zero thickness for derivation of stiffness matrix. It is desirable to introduce the rotation

stiffness in the joint to consider the combination of the slip and the rotation.

TABLE 2.9

Chronology of development of joint elements

Reference, date	Geometry			No thickness	Rotation stiffness	Dilation	Strain softening	Fluid Flow	Quadratic
	Plane	Axi-symmetric	Three dimensional						
(1)	(2)	(3)	(4)	(5)	(6)	(7)	(8)	(9)	(10)
59,1968	*			*					
107,1970			*	*					
71,1971	*		*				*		
123,1971	*			*				*	
70,1971	*			*		*[a]	*		
153,1972	*		*	*					
141,1972	*			*		*[a]	*		
56,1972	*			*		*[a]	*[c]		
52,1973	*[b]	*				*[a]			
51,1974	*			*				*	
122,1975	*			*					*
150,1976	*								*
72,1976	*							*	
58,1977	*			*	*	*[a]	*		
73,1978	*			*	*	*[a]	*		*
68,1979	*			*	*	*[a]			
167,1981	*			*		*[a]			
159,1981	*		*			*[a]			

$*^a$ = No explicit coupling between opening and reclosing tendencies.

$*^b$ = Element singular at some orientations.

$*^c$ = Iteration by load transfer.

It is absolutly essential to include the dilational effect to obtain the realistic results. Most joint elements are linear having only two nodes along the given side, however recently a few quadratric elements are also developed. The most notable joint elements which are in vogue for design analysis are described below.

(i) Goodman, Taylor and Brekke (1968) proposed one of the commonly used interface element in soil. The joint element formulation is derived on the basis of relative nodal displacements of surrounding interface element(Fig.2.38).

(ii) Zienkiewicz et al (1970) used an isoparametric finite element formation for an interface element which is treated essentially like a solid element.

(iii) Ghaboussi, Wilson and Isenberg (1973) proposed a formulation which is derived by considering relative motion between surrounding solid elements as independent degree of freedom.

(iv) Katona et al (1981) derived an interface model from the virtul work principle modified by appropriate constraint conditions. Various deformation modes at the interface are also incorporated in this formulation.

(v) Herrmann (1978) presented an algorithm for an interface element similar to Goodman et al element in which sliding and debonding modes have been considered.

(vi) Heuze and Barbour (1982) proposed a dilatant joint model for axisymmetrical interface formulated in two ways (a) starting from a strain displacement relation with a vanishing joint thickness (b) from a transversely isotropic right angle in a material with zero poission's ratio and vanishing element thickness.

(vii) Desai, Zaman, Lightner and Siriwardane (1984) developed a thin layer element for interface in joints, considering the various deformation modes such as no slip, slip, debonding and rebonding with special incorporation for thickness of the thin layer element (Fig. 2.39 and 2.40).

2.8.0 CONCLUDING REMARKS

The apprisal of various investigations is that the behaviour of jointed rock is complex and depends on many factors ranging from mineral genesis to the phenomena resultant not only from physical conditions but also from loading conditions. However, one single principal phenomenon recognized is dilatancy which appear to largely influence the shearing behaviour of jointed rocks. In order to understand the behaviour it is imperative to separate the total frictional behaviour from the dilational effects. The need, however, is to have a parameter capable of providing the dilational quantity.

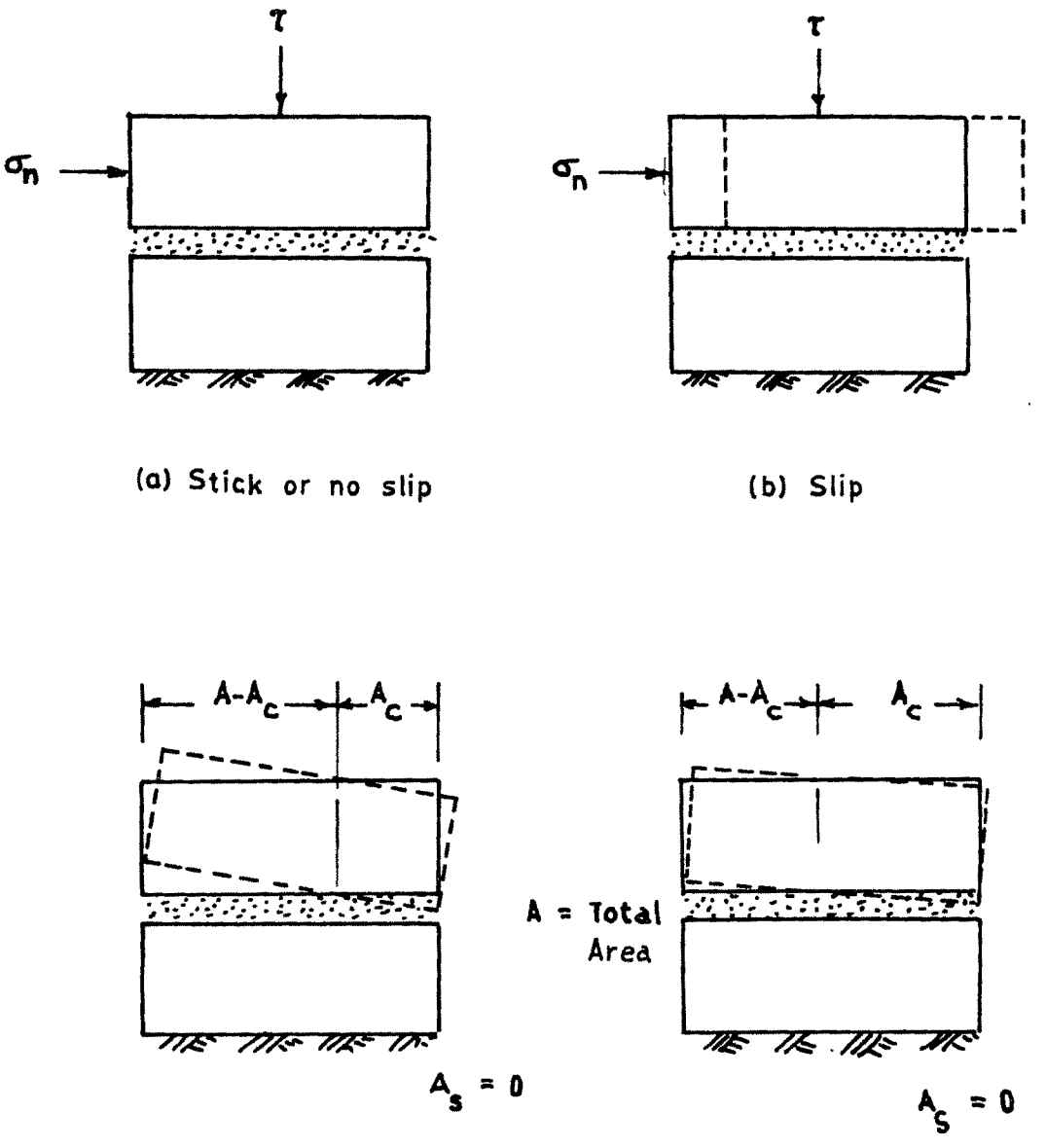

FIG.2-39 SCHEMATIC OF MODES OF DEFORMATION AT INTERFACE

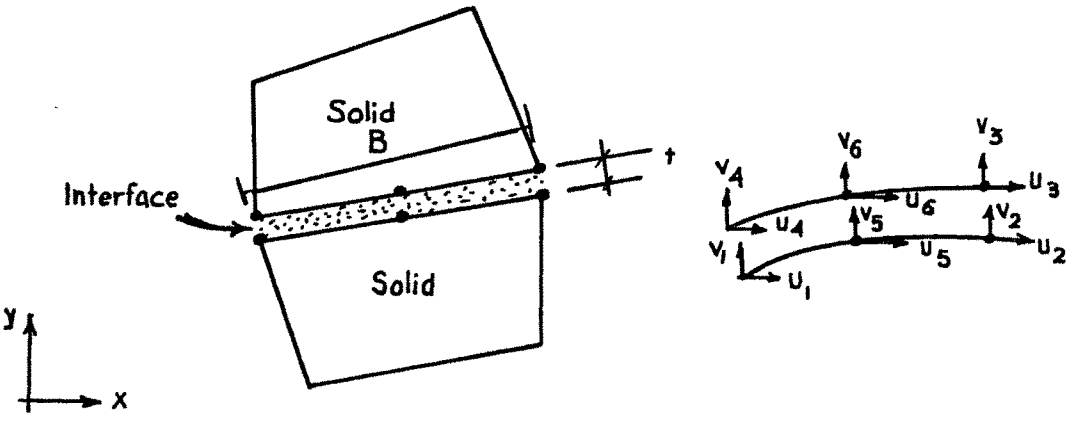

(a) Two-dimensional

B = (average) contact dimension

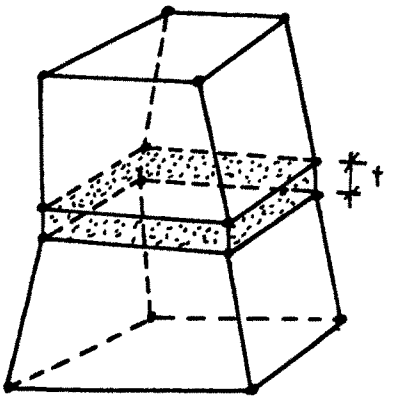

(b) Three-dimensional

FIG. 2-40 THIN LAYER INTERFACE ELEMENT